



Australian  
National  
University

ANU Research Repository

<https://digitalcollections.anu.edu.au/>

THE PUBLISHER OF "*the FEBS Journal*" DOES NOT PERMIT DEPOSIT OF THE PUBLISHERS' VERSION/PDF OF ARTICLES IN INSTITUTIONAL REPOSITORIES.

This is the accepted version of the following article: *the FEBS Journal* 281.6 (2014): 1517–1533, which has been published in final form at

<http://onlinelibrary.wiley.com/doi/10.1111/febs.12729/abstract>

**Binding mode of the activity-modulating C-terminal segment of NS2B to NS3 in the dengue virus NS2B-NS3 protease**

Laura de la Cruz,<sup>1</sup> Wan-Na Chen,<sup>1</sup> Bim Graham,<sup>2</sup> Gottfried Otting<sup>1,#</sup>

<sup>1</sup> Research School of Chemistry, Australian National University, Canberra, ACT 0200, Australia

# Corresponding author

phone: +61 2 61256508

fax: +61 2 61250750

e-mail: [gottfried.otting@anu.edu.au](mailto:gottfried.otting@anu.edu.au)

<sup>2</sup> Medicinal Chemistry and Drug Action, Monash Institute of Pharmaceutical Sciences, Parkville VIC 3052, Australia

Short title: Structure of the dengue virus NS2B-NS3 protease

Keywords:

Dengue virus; NMR spectroscopy; NS2B-NS3 protease; paramagnetic tags; pseudocontact shifts

## **Abstract**

The two-component dengue virus NS2B-NS3 protease (NS2B-NS3pro) is an established drug target but inhibitor design is hampered by uncertainties about its three-dimensional structure in solution. Crystal structures reported very different conformations for the functionally important C-terminal segment of the NS2B co-factor (NS2Bc), indicating open and closed conformations in the absence and presence of inhibitors, respectively. An earlier nuclear magnetic resonance (NMR) study in solution indicated that a closed state is the preferred conformation in the absence of an artificial linker engineered between NS2B and NS3pro. To obtain direct structural information on the fold of unlinked NS2B-NS3pro in solution, we tagged NS3pro with paramagnetic tags and measured pseudocontact shifts by NMR to position NS2Bc relative to NS3pro. NS2Bc was found to bind to NS3pro in the same way as reported in a previously published model and crystal structure of the closed state. The structure is destabilized, however, by high ionic strength and basic pH, showing the importance of electrostatic forces to tie NS2Bc to NS3pro. Narrow NMR signals previously thought to represent the open state are associated with protein degradation. In conclusion, the closed conformation of the NS2B-NS3 protease is the best model for structure-guided drug design.

## Introduction

Dengue virus is a health burden that sends almost 100 million people to clinics every year [1] and puts an estimated 40% of the world population at risk especially in the tropical and sub-tropical regions [2,3]. The infection involves the translation of the flavivirus RNA genome into a poly-protein, which must be cleaved into several individual components. The N-terminal part of the non-structural protein 3 (NS3) encodes a serine protease, NS3pro, which is required for cleavage of the poly-protein. This makes NS3pro a prime drug target [4]. Its activity towards peptide substrates is boosted about 3300- to 7600-fold by the presence of a second viral protein, NS2B, which comprises about 40 residues [5]. The NS2B-NS3 proteases of the dengue serotypes 1-4 are closely related to each other (Fig. S1) and to the NS2B-NS3 protease from the West Nile virus (WNV; about 40% sequence identity). The present work focuses on the NS2B-NS3 protease of the dengue virus serotype 2, which is the most studied serotype.

The wild-type poly-protein contains a recognition site for the NS2B-NS3 protease between NS2B and NS3 [6]. To stabilize the protein, the most widely used construct of the NS2B-NS3 protease contains a 47-residue segment of NS2B fused to the N-terminus of NS3pro via an artificial Gly<sub>4</sub>-Ser-Gly<sub>4</sub> linker. This and similar constructs retain the activity of the protease [7] and have been used for crystal structure determinations [8,9], NMR spectroscopic studies [10,11] and ligand binding studies [12-28]. In the following we refer to this construct as DENpro (WNVpro for the corresponding construct from WNV). We use the name DENp for an alternative construct that is devoid of the covalent linkage between NS2B and NS3pro. The distinction is important, because the functionally important NS2B co-factor has been reported to assume very different conformations in DENpro and DENp (Fig. 1).

Crystal structures of DENpro and WNVpro in the absence of inhibitors revealed an open conformation [8,29], in which the N-terminal part of the NS2B co-factor inserts into the N-terminal  $\beta$ -barrel of the NS3 protease, but the C-terminal segment of NS2B (NS2Bc, corresponding to the segment Glu66-Leu95 in DENpro serotype 2) is located far from the substrate-binding site of NS3pro. We refer to the structures with NS2Bc

far from the active site of NS3pro as the “open state” (Fig. 1A). In contrast, structures determined in the presence of inhibitors displayed NS2Bc forming a  $\beta$ -hairpin that lines the substrate-binding site [8,29-32]. We refer to this conformation as the “closed state” (Fig. 1B). In view of the importance of NS2Bc for full proteolytic activity of the proteases [5,33-37], the closed conformation is assumed to represent the enzymatically active structure. As expected for homologous proteins, the closed conformations reported for DENpro and WNVpro in the presence of inhibitors are very similar [8,30]. Remarkably, also the crystal structures of the open conformations without inhibitors are very similar [8,29].

In solution, NMR experiments unambiguously showed that DENpro can assume the closed conformation in the presence of inhibitor **1** (Fig. S2A)[11]. In the absence of an inhibitor, however, not all signals could be observed, indicating extreme broadening of the NMR resonances of DENpro due to conformational exchange. A similar situation was observed in the case of WNVpro: the protein assumes the closed conformation in the presence of inhibitors, but the disappearance of signals in the absence of inhibitors indicates conformational exchange. NMR experiments showed that the closed conformation is more highly populated in either case [38].

A recent study investigated a construct of DENp produced by co-expression of NS2B and NS3pro without a covalent link between both proteins [39]. Significant differences to the earlier results obtained with DENpro were found. Importantly, no NMR signals were reported to be missing in the absence of inhibitors, allowing more complete resonance assignments and thus the measurement of secondary chemical shifts,  $^{15}\text{N}$ -relaxation rates and PREs from a spin-label attached to NS2Bc. These data indicated that NS2B may exist in a conformation similar to the closed form of DENpro, but structural details were not obtained.

The present study presents direct structural information for a related unlinked NS2B-NS3pro construct, using pseudocontact shifts induced by different paramagnetic lanthanide ions attached at different sites. The data fully support the structure of the closed state detected previously in the presence of inhibitors [11,30], but NS2Bc is found to undergo conformational exchange that becomes more pronounced at increased

pH and ionic strength, without appreciably dissociating from NS3pro even under conditions of high salt. Evidence is presented that a set of very narrow signals at chemical shifts characteristic of random coil conformations previously attributed to open conformations [10,38] instead signifies degraded protein. The results show that the structure and dynamics of the dengue NS2B-NS3 protease are much more closely related to the corresponding protease from the West Nile virus than implied by previous analyses.

## **Results**

### **Protein production**

DENp was expressed as a single polypeptide chain to produce NS2B and NS3pro in equimolar ratio. SDS-PAGE showed that the autoproteolytic cleavage site was quantitatively cleaved in the course of protein expression and purification, regardless of whether the protein was produced by cell-free synthesis or *in vivo* (Fig. S2C). ESI mass spectrometry of DENp selectively labelled with <sup>15</sup>N-isoleucine showed two peaks of molecular mass 6670 and 20753 (calculated: 6671 and 20757 for NS2B and NS3pro, respectively). DENp was enzymatically active (Fig. S3).

### **DENp assumes the closed conformation**

The <sup>15</sup>N-HSQC spectrum of DENp selectively labelled with <sup>15</sup>N-isoleucine (Fig. 3A) was strikingly similar to that of DENpro in the presence of inhibitor **1** (Fig. 3C). The improved spectral quality of DENp is in line with earlier observations, where a similar unlinked construct of the NS2B-NS3 protease was shown to produce better NMR spectra than the DENpro construct [39]. We previously established by pseudocontact shifts from multiple lanthanide binding sites [11] that the structure of DENpro with bound inhibitor **1** assumes the closed conformation as observed in the crystal structure 3U1I [30]. The conservation of chemical shifts observed for the isoleucine residues in DENp without inhibitor (Fig. 3A) and DENpro with inhibitor **1** (Fig. 3C) thus indicates that DENp assumes the closed conformation too. Apart from small differences in

chemical shifts expected to arise from the presence or absence of the inhibitor and the covalent linker peptide (for example, Ile36, which is close to the active site, changes its chemical shift between DENp without inhibitor and DENpro with inhibitor **1**), there are pronounced differences in peak intensities. For example, the cross-peaks of Ile78\* and Ile86\* in NS2B and Ile165 in NS3pro were unexpectedly weak. Effects of this magnitude can only be explained by exchange broadening, which we attribute to conformational exchange of the  $\beta$ -hairpin of NS2Bc. Ile165 is buried in the C-terminal  $\beta$ -barrel of NS3pro which binds NS2Bc in the closed conformation. Sensitivity of the C-terminal  $\beta$ -barrel to the state of NS2Bc has been reported earlier [11].

Remarkably, greater spectral differences are observed between DENpro without inhibitor (Fig. 3B) and either DENpro with inhibitor **1** (Fig. 3C) or DENp without inhibitor (Fig. 3A). For example, the resonance of Ile123 is strongly affected in Fig. 3B and there are no signals of Ile165, Ile67\* and Ile73\* that would be expected for the closed conformation. Another notable feature of the spectra of Fig. 3B and C is a set of narrow signals for isoleucine residues of NS2B at  $^1\text{H}$  chemical shifts characteristic of an unfolded polypeptide chain (8.1 – 8.3 ppm). In early NMR studies of DENpro, these signals were very intense and assigned to NS2B by systematic site-directed mutagenesis [10]. In the spectrum of Fig. 3B, however, these cross-peaks are much weaker than those of NS3pro. Having repeated these preparations and NMR measurements multiple times, we found the intensity of these NS2B signals to vary between different sample preparations and not to change when inhibitor **1** was added to the sample. Notably, previous experiments of selectively  $^{15}\text{N}$ -Ser labelled samples of DENpro without inhibitor displayed weak  $^{15}\text{N}$ -HSQC cross-peaks of the serine residues of NS2B at the chemical shifts of the closed conformation, with little evidence of serine residues at random coil chemical shifts [11]. We conclude that the cross-peaks of isoleucine residues of NS2B at random coil chemical shifts stem from degradation of the NS2B-NS3pro complex, possibly resulting in free NS2B, which is known to be soluble whereas NS3pro is insoluble. In agreement with this interpretation, the corresponding set of narrow peaks in selectively  $^{15}\text{N}$ -isoleucine-labelled DENp grew noticeably in height already after 4 hours at 25 °C in step with protein precipitation. This conclusion

supersedes our earlier interpretation that the random coil signals of NS2B represent the open conformation of NS2B in the NS2B-NS3pro complex [11,38].

Discounting the signals from the degraded protease, there is no second set of isoleucine cross-peaks that would indicate the existence of the open conformation in either DENp or DENpro. Instead, the open conformation may be manifested in the apparent absence and weakness of some of the isoleucine cross-peaks in the  $^{15}\text{N}$ -HSQC spectrum, which indicates excessive line broadening arising from conformational exchange. To rule out line broadening due to chemical exchange of the amide protons with the water, we performed a control experiment to assess the amide proton exchange rates. The experiment used selective excitation of the water resonance followed by a mixing time to allow magnetisation transfer by chemical exchange followed by the  $^{15}\text{N}$ -HSQC pulse sequence to record the amide cross-peaks arising from chemical exchange with water. The spectrum was recorded of selectively  $^{15}\text{N}$ -Ile/ $^{15}\text{N}$ -Ser-labelled DENp. The scarcity of observable cross-peaks (Fig. 4C) confirmed that exchange with the water resonance was unimportant even at pH 7.5, where exchange with water is more pronounced than at lower pH [40]. Weak cross-peak intensities in the  $^{15}\text{N}$ -HSQC spectra of Fig. 3 are thus indicative of conformational rather than chemical exchange broadening.

### **Structural analysis of DENp by pseudocontact shifts**

While the overall conservation of chemical shifts between DENp and DENpro indicates structural conservation, we sought more direct evidence by measuring pseudocontact shifts (PCS) in DENp. To do this without mutations in the critical NS2Bc segment, we prepared three different single-cysteine mutants for labelling with paramagnetic C1- and C2-lanthanide tags. The mutation sites corresponded to the sites A, B and C (Ala57\*Cys, Ser34Cys and Ser68Cys) used previously to establish the closed conformation of DENpro in the presence of the inhibitor **1** [11]. In the study of DENpro [11], on average larger PCSs were obtained with the C2 than with the C1 tag. Therefore, we recorded data with the C1 tag only for mutant B, which delivered the largest number of PCSs for NS2B. For all three mutants, PCSs were measured with  $\text{Tm}^{3+}$  and  $\text{Tb}^{3+}$  tags. Fig. 5

shows examples of PCSs measured for mutant B with the C1-Tb<sup>3+</sup> tag in DENp without inhibitor and compares them with corresponding PCSs measured for DENpro with inhibitor **1**. Fig. 6 shows an overview of all the PCSs that could be resolved for both DENp and DENpro with different tags. Clearly, the PCSs measured for DENp and DENpro were very similar throughout, including, in particular, resonances of NS2Bc. The PCSs thus provide very clear evidence that both NS3pro and NS2B predominantly assume the closed conformation in DENp. The model of the closed conformation of DENpro established by PCSs [11] is very similar to the crystal structure of the serotype 3 NS2B-NS3 protease determined in the presence of an inhibitor [30] with a backbone rmsd of 0.7 Å.

### **Conformational exchange of NS2B**

DENp and DENpro display more intense <sup>15</sup>N-HSQC cross-peaks in the presence of the inhibitor **1**. Fig. 7 shows a quantitative assessment of the relative peak heights of samples selectively labelled with <sup>15</sup>N-Ser and <sup>15</sup>N-Ile in the absence and presence of inhibitor. Clearly, signals from NS2B are more strongly affected than those of NS3 and DENpro suffers more from exchange broadening than DENp, including residues 123 to 165 of NS3pro. This observation reinforces the conclusion that the C-terminal β-barrel, which harbours those residues, senses the conformational exchange of NS2B. Notably, residual exchange broadening persists in DENp in the absence of inhibitor for NS2B and also for Ile139 in NS3.

While it is common that binding of an inhibitor rigidifies a protein structure, it is remarkable that the low-molecular weight inhibitor used here achieves this for NS2B, as the inhibitor is too small to form direct contacts with NS2B. Based on mutation and mass spectrometry data, the inhibitor hydrolyses upon binding, leaving only a *p*-guanidino-benzoyl moiety behind that is covalently bound to Ser135 [11]. We hypothesized that the positive charge of the guanidino group helps to tie NS2Bc to NS3, as the C-terminal β-hairpin of NS2B is highly negatively charged owing to the presence of Glu80 and Asp81 and four additional glutamates at the C-terminus of NS2B (Fig. S1).

If electrostatic interactions are important, the association of NS2B to NS3 should be weakened by high salt concentrations. Furthermore, the association should be weakened at higher pH, when His51 in the active site loses its positive charge.

Fig. 4 shows that the  $^{15}\text{N}$ -HSQC cross-peaks of many residues became significantly weaker at pH 7.5 compared to pH 6.5 and that this loss in intensity was not due to fast proton exchange with the water. As expected, the effect was observed equally for DENp and DENpro, whereas the signals retained their intensities in the presence of the inhibitor **1** (Fig. 8). The presence of 300 mM NaCl at pH 6.5 weakened the signal of Ile78\* in a selectively  $^{15}\text{N}$ -Ile labelled sample (Fig. S5). A uniformly  $^{15}\text{N}$ -labelled sample confirmed this result, i.e. most cross-peaks of NS2Bc were significantly weaker or absent at 300 mM NaCl, whereas the cross-peaks from NS3pro were much less affected (Fig. 9B), except for some cross-peaks of amides in NS3pro that are sufficiently close to NS2B to sense its conformational exchange (Fig. 9C). These results indicate that the association of NS2Bc to NS3pro is indeed stabilized by electrostatic attraction.

In view of the open conformations found in crystal structures of DENpro and WNVpro [8,29], it is plausible that the pH- and salt-dependent conformational exchange of NS2B in DENp arises from temporary dissociation of NS2Bc from NS3pro, leading to the open conformation. As stated above, however, the PCSs measured for NS2B were in full agreement with the closed conformation. PCSs readily average to zero for flexible polypeptide chains, so that any disordered open conformation would not contribute to PCSs of NS2B and, therefore, the average PCSs of closed and open conformations would become smaller for increasing populations of open conformations. The similarity in PCSs observed in DENp without inhibitor and DENpro with inhibitor **1** (Fig. 6) indicates that, at pH 6.5 and low ionic strength, DENp does not populate open conformations to any significant extent.

In a fast equilibrium between open and closed conformations, a minor population of open conformation should be manifested in changes in chemical shifts, whereas a slow equilibrium would result in new cross-peaks for the open conformation. As the protein chemical shifts are very highly conserved between pH 6.5 and pH 7.5 without any new peaks appearing at pH 7.5 (Fig. 4A and B), open conformations cannot be highly

populated at the higher pH. Nonetheless, many signals broaden significantly at pH 7.5. A more complete picture was obtained by using uniformly  $^{15}\text{N}$ -labelled DENp. The comparison of Figs 9 and 10 shows that high pH and high salt predominantly affect the residues of NS2Bc and nearby residues of NS3pro, suggesting that the electrostatic attraction of NS2Bc to NS3pro is weakened at increased pH. This result may be explained by a loss of charge of the side chain of His51. If the exchange broadening observed at high salt and high pH arises from small populations of open conformations, DENpro would be expected to be more sensitive than DENp. This is indeed the case (Fig. 4).

The chemical shifts of DENp changed slightly in the presence of high salt, raising the possibility that this effect could be attributed to a greater population of open conformations. It was difficult, however, to assess the amount of open population, as all NS2Bc resonances were too broad to be observable (Fig. 9A) and Ser70\* and Ser71\* were the last residues of NS2B for which amide cross-peaks could be detected in uniformly  $^{15}\text{N}$ -labelled DENp at high salt. Their PCSs generated by the C2-Tb tag attached to a cysteine residue at site B (Fig. S6) changed slightly at high salt, but other PCSs in NS3pro also changed, reflecting a small change in the average location and orientation of the paramagnetic tag relative to the protein. This effect is not unexpected, as the lanthanide tags used were charged and thus sensitive to attractive and repulsive forces from the charged amino acid side chains on the protein surface. Using all observable PCSs to fit  $\Delta\chi$  tensors yielded good correlations between back-calculated and experimental PCSs, including for residues 70\* and 71\* (Fig. S7). The PCS data thus indicate that Ser70\* and Ser71\* of NS2Bc retain their closed-state association with NS3pro even at high ionic strength. In contrast, the more C-terminal residues of NS2Bc are subject to substantial conformational exchange, which may or may not include dissociation from NS3pro. Clearly, however, the open conformation observed in the crystal structure [8] can be populated to a very small extent only (less than 10%).

## Discussion

## **Open and closed conformations**

The question of open and closed conformations in the dengue virus and West Nile virus proteases has been vexed ever since their first observation in crystal structures [8]. As NS2B greatly increases the activity of the proteases [5,41], it would be attractive to prevent the association of NS2Bc with the substrate-binding site by a drug molecule. Inhibitor designs for DENpro have used either conformation as template [14,17,19,20,23,26,42-52]. For both WNVpro and DENpro, the presence of low molecular weight inhibitors greatly improves the quality of the NMR spectra [11,38,44,53-55]. For WNVpro, however, the NMR experiments clearly showed that the closed conformation is predominant in solution regardless of the presence of an inhibitor [38]. The situation was thought to be different for DENpro, as very narrow signals indicative of NS2Bc in a random coil conformation were observed with high intensities in the absence of inhibitors [10]. In the course of the present study, these signals proved to be little reproducible in intensity, with some sample preparations showing hardly any evidence for them at all. Furthermore, they were insensitive to the addition of inhibitor **1**. These observations clearly identify these signals as degradation products and eliminate them as evidence for a predominantly open conformation, in contrast to our previous interpretation [38]. Heterogeneity in DENpro sample preparations has been reported previously [56] but the evidence for open conformations in solution is not clear-cut.

Kim *et al.* reported earlier this year [39] that an unlinked construct of the NS2B-NS3 protease yields better NMR spectra than the original linked DENpro construct. They also used NMR spectroscopy to establish that the unlinked protease most likely assumes the closed conformation. The key observations were (i) that the <sup>15</sup>N-relaxation times of the NS2Bc resonances were overall comparable to those of NS3pro, showing that the mobility of NS2Bc is not greatly enhanced compared to that of NS3pro in agreement with the closed state, and (ii) that paramagnetic relaxation enhancements (PRE) could be resolved for seven of the backbone amides in the globular part of the protease in a cysteine mutant with a nitroxide radical attached to residue 75 of NS2B. The PREs were also in agreement with the closed conformation and could not be explained by the open conformation of the crystal structure 2FOM [8]. In addition,

approximate boundaries of secondary structure were derived from the chemical shifts of NS2B that are in agreement with the  $\beta$ -hairpin structure found for NS2Bc in the crystal structure 3U1I of the closed conformation [30].

The crystal structures of DENpro and WNVpro indicate that the association between NS2Bc and NS3pro is weak, as the closed conformation has only ever been observed in the presence of an inhibitor. Even with the strongly binding inhibitor aprotinin, a co-crystal structure of DENpro showed no electron density for NS2Bc, indicating that it is disordered [30]. Nonetheless, the crystal structures of WNVpro [29] and DENpro from serotype 1 [9] showed that the  $\beta$ -hairpin structure of NS2Bc forms readily also when NS2Bc is dissociated from NS3pro. It is thus conceivable that, in solution, the  $\beta$ -hairpin structure forms and associates non-specifically with NS3pro. The NMR data of Kim *et al.* [39] could not discern this situation from the well-defined closed conformation observed with inhibitors [11,30], as distance restraints to nitroxide tags are difficult to quantify. In addition, the hydrophobicity of the tag could influence the interaction with NS3pro.

The pseudocontact shifts observed in the present study using multiple tags at multiple sites unambiguously establish that the dengue virus NS2B-NS3pro enzyme from serotype 2 assumes the closed conformation as observed in the crystal structure 3U1J [30], when the covalent linkage between NS2B and NS3pro is broken. At the same time, however, broad and missing NMR signals show that NS2Bc retains increased dynamics which increase with increasing salt and pH.

### **Conformational exchange**

All backbone amide groups with the same relaxation times should display  $^{15}\text{N}$ -HSQC cross-peaks of the same intensity, while increased relaxation rates reduce the cross-peak intensities by broadening the signals and because of loss of magnetisation by fast relaxation during the spin-echo periods of the experiment. As no relaxation mechanism can compete with the line broadening effects from chemical exchange, the weak signal intensities observed in the spectra of DENpro and DENp must arise from exchange broadening. As hydrogen exchange with water is inefficient at pH 7.5, conformational

exchange remains the only plausible mechanism for the loss of cross-peak intensities.

It is tempting to identify the exchange broadening with an exchange between open and closed conformations. Our current results show that the broadening becomes more pronounced by increasing the pH or the salt concentration, showing that the interaction between NS2Bc and NS3pro has a significant electrostatic component. Even in the presence of 300 mM NaCl, however, when most signals of NS2Bc become unobservable, the pseudocontact shifts of the last backbone amides of NS2Bc that we were able to resolve (Ser70\* and Ser71\*), induced by a C2-Tb tag at site B, were not at all reduced, contrary to expectations when NS2Bc fully dissociates from NS3pro and assumes a random position relative to the tag. This suggests that the exchange broadening arises from exchange between different conformations of the  $\beta$ -hairpin of NS2Bc while it is bound or from its selective dissociation from NS3pro. In either case, the fully open conformations reported in crystal structures are not the predominant form in solution even under conditions that promote conformational exchange of NS2Bc.

The  $^{15}\text{N}$ -Ile labelled DENpro construct shows no cross-peaks of NS2Bc in the closed conformation (Fig. 3B), indicating that the Gly<sub>4</sub>-Ser-Gly<sub>4</sub> linker enhances the conformational exchange of NS2Bc. Nonetheless, weak cross-peaks at chemical shifts characteristic of the closed conformation have been observed in  $^{15}\text{N}$ -Ser labelled samples [11], showing that the closed conformation is populated even in DENpro. As there are no cross-peaks of NS2Bc in the spectrum of Fig. 3B that can be assigned to the intact NS2B-NS3 protease, it is hard to tell whether the closed or open state is more highly populated in DENpro. Certainly, the conformational state of DENpro is more sensitive to high pH, as cross-peaks from NS3pro disappear more readily at pH 7.5 than the corresponding signals in DENp (Fig. 8).

### **Pseudocontact shifts for structure analysis**

The present study illustrates the power of PCSs induced by lanthanide tags. Traditionally, most NMR studies collect long-range structure restraints by measuring PREs from site-specifically attached nitroxide spin-labels. PREs, however, can also arise from intermolecular interactions and artificial interactions can be promoted by the

hydrophobic nature of conventional nitroxide spin-labels. In contrast, the PCS effect can be measured over greater distances, allowing attachment of the tag at a site far from the site of interest where it causes minimal perturbations, and non-specific intermolecular interactions do not generate PCSs [57]. The PCSs proved particularly valuable in the case of DENp at high salt, where the signals of NS2Bc were either missing or strongly attenuated due to conformational exchange. This demonstrates how PCSs can provide structural information even under adverse conditions, where NMR signals can be observed only for isolated residues because of peak broadening, low protein concentrations or unstable preparations.

### **Dissociation of NS2Bc from NS3pro**

In contrast to DENpro which is stable against degradation at room temperature, our DENp construct precipitated rapidly during the NMR measurements. Precipitation was even faster at high ionic strength, limiting the measurement time for each sample to about 4 hours. A possible explanation for this effect is that the absence of the linker between NS2B and NS3pro facilitates the dissociation of NS2B, as NS3pro on its own is insoluble.

Could the open conformations observed in crystal structures be caused by the crystallization conditions used? It is well known that exchange with small populations of alternate conformations can be sufficient to broaden NMR signals beyond detection and that crystallization conditions can select unusual conformations. Interestingly, serotype 2 DENpro without inhibitor was crystallized at pH 8.5 and 48 °C [8], conditions which could promote dissociation of NS2Bc from NS3pro. The open conformation of WNVpro crystallized at pH 7.5 and 25 °C [29], but it was obtained of the His51Ala mutant, which could have weakened the binding of NS2Bc to NS3pro. The open conformation of serotype 1 DENpro was of the wild-type protein crystallized at pH 7.5 and 20 °C [9]. Based on our present data, these conditions would not promote dissociation of NS2Bc from NS3pro, but the difference in amino acid sequence may confer different properties to this particular protein, favouring the association between the NS2Bc segments from different protein molecules as observed in the crystal structure.

## **Conclusion**

The present results unequivocally demonstrate that the serotype 2 dengue virus NS2B-NS3 protease in solution predominantly assumes the closed conformation in the absence of inhibitors and that any open conformation is hardly populated. This has obvious and important implications for the choice of structural templates in the rational design of inhibitors.

## **Experimental procedures**

### **Materials**

Two different dengue 2 NS2B-NS3pro constructs were used in the present work. The first construct was the traditional construct used earlier for structural and functional work [7,8,11], comprising 255 residues with a (Gly)<sub>4</sub>-Ser-(Gly)<sub>4</sub> linker between NS2B (47 residues) and NS3pro (185 residues). In addition, it contained a His<sub>6</sub>-tag at the C-terminus and the T7 gene 10 N-terminal peptide MASMTG at the N-terminus followed by a two-residue cloning artifact (Leu-Glu), resulting in a 27 kDa protein. In this construct, NS2Bc comprises the segment from Glu66\* to Leu95\* (to discriminate between NS2B and NS3 residues, residue numbers of NS2B are marked by an asterisk throughout this text). We refer to this construct as DENpro. The second construct was the same as the first construct, except that the (Gly)<sub>4</sub>-Ser-(Gly)<sub>4</sub> sequence in the linker between NS2B and NS3pro was replaced by the protease recognition sequence EVKKQR that precedes NS3 in the wild-type poly-protein (Fig. 2A and B). We refer to this construct as DENp.

DENpro and DENp samples were prepared either by cell-free protein synthesis from PCR-amplified DNA [10] or by high-cell density *in vivo* expression [58]. Cell-free protein synthesis used the high-copy number plasmid pRSET-6d-DEN2 CF40GlyNS3pro as the template for PCR-amplification [8,59]. S30 cell extracts were prepared in-house from *E. coli* strains Rosetta::λDE3/pRARE and BL21 Star::λDE3 [42], including concentration with polyethylene glycol 8000. <sup>15</sup>N-labelled amino acids were purchased from Cambridge Isotope Laboratories and ISOTEC. Synthetic

oligonucleotides were purchased from IDT-DNA Technologies and Geneworks. PCRs were performed using *Vent* DNA polymerase (New England Biolabs). PCR products were purified using the QiaQuick PCR purification kit (Qiagen).

Single-cysteine mutants were prepared by *in vivo* expression experiments using the same gene constructs as cell-free expression but inserted into the pETMCSI T7 expression vector [60] and transformed into the *E. coli* strain Rosetta:: $\lambda$ DE3/pRARE.

The C1- and C2-compounds for tagging with lanthanides were synthesized as described [61].

### **Cell-free protein synthesis**

Production by cell-free synthesis allowed selective labelling with  $^{15}\text{N}$ -labelled amino acids without significant isotope scrambling [62] and the rapid production of site-specific mutants [10]. Samples of DENp were synthesized in a cell-free *E. coli* coupled transcription-translation system using a previously described protocol [63,64].  $^{15}\text{N}$ -labelled isoleucine was used in the cell-free reaction mixture. Wild-type DENpro was synthesized using the pRSET-DEN2 CF40GlyNS3pro plasmid at a concentration of 16  $\mu\text{g}/\text{ml}$  of reaction mixture. Mutant DENpro was synthesized using re-annealed DNA at a concentration of 20  $\mu\text{g}/\text{ml}$  of reaction mixture. Each synthesis was performed in two identical parallel reactions, each using a reaction volume of 2 ml in 20 ml of outer buffer and proceeding for 14-15 h at 30 °C.

The S30 extract used for the expression of selectively  $^{15}\text{N}$ -serine labelled samples was reduced with sodium borohydride to suppress cross-labelling by transaminases as described previously [65]. 100-150  $\mu\text{M}$  NMR samples were obtained from three 2.5 ml reactions in 25 ml of outer buffer at 30 °C in overnight reactions (14-15 h).

### **Protein purification**

Following synthesis, the protein samples were purified using IMAC Ni-NTA spin columns. The columns were equilibrated with binding buffer (50 mM HEPES, 300 mM NaCl, 10 mM imidazole at pH 7.5), loaded with the sample, washed five times with wash buffer (50 mM HEPES, 300 mM NaCl, 30 mM imidazole, pH 7.5), and eluted

with elution buffer (50 mM HEPES, 300 mM NaCl, 300 mM imidazole, pH 7.5). The purified protein was dialyzed extensively against NMR buffer (20 mM MES, pH 6.5, 50 mM NaCl or 20 mM Tris.HCl, pH 6.9 or pH 7.5, 50 mM NaCl). Samples at higher salt concentrations (300 mM NaCl) were prepared by dialysis against buffers with correspondingly increased salt concentration. Samples were concentrated using a Centricon-4 ultrafilter MWCO-10 kDa concentrator (Amicon) to final volumes of 0.5 ml for samples at low salt concentration in 5 mm NMR tubes and 0.2 ml for samples at high salt concentration in 3 mm NMR tubes. The protein concentrations at low and high salt were 0.2 and 0.7 mM, respectively.

### **Tagging reaction**

C1- and C2-tags loaded with Tb<sup>3+</sup>, Tm<sup>3+</sup> or Y<sup>3+</sup> (Fig. S2) were attached to the single cysteine mutants of DENp by adding the protein to a three-fold excess of the respective metal complexes of C1 or C2 and incubating at room temperature for several hours. Excess low-molecular weight reactants and products were removed by washing with NMR buffer.

### **NMR spectroscopy**

All NMR spectra were recorded at 25 °C on Bruker 600 and 800 MHz NMR spectrometers equipped with cryoprobes. NMR spectra were recorded in NMR buffer unless indicated otherwise. *p*-nitrophenyl-*p*-guanidino benzoate (**1**; Fig. S2A) was used as the inhibitor [66]. The inhibitor was added in five-fold molar excess to the protein using a 100 mM stock solution in DMSO-d<sub>6</sub>. A spectrum for measuring chemical exchange between water and amide protons was recorded using the CLEANEX-PM pulse sequence [67].

### **Pseudocontact shifts**

PCSs were measured as the <sup>1</sup>H chemical shifts of backbone amides observed in <sup>15</sup>N-HSQC spectra of paramagnetic samples minus those observed for diamagnetic samples. The PCSs were generated by a lanthanide ion with non-isotropic magnetic

susceptibility. For each nuclear spin, the PCS (measured in ppm) depends on its polar coordinates  $r$ ,  $\theta$  and  $\varphi$  with respect to the principal axes of the  $\Delta\chi$  tensor:

$$\Delta\delta^{\text{PCS}} = \frac{1}{12\pi r^3} \left[ \Delta\chi_{\text{ax}} (3\cos^2\theta - 1) + \frac{3}{2} \Delta\chi_{\text{rh}} \sin^2\theta \cos 2\varphi \right] \quad (1)$$

where  $\Delta\chi_{\text{ax}}$  and  $\Delta\chi_{\text{rh}}$  denote, respectively, the axial and rhombic components of the magnetic susceptibility tensor  $\chi$  [68], and the  $\Delta\chi$  tensor is defined as the  $\chi$  tensor minus its isotropic component. Equation 1 shows that PCSs can be positive or negative, depending on the position of the nuclear spin with respect to the coordinate system defined by principal axes of the  $\Delta\chi$  tensor. For mobile polypeptide chains, PCSs easily average to zero.

### **Acknowledgements**

We thank Dr Siew-Pheng Lim at the Novartis Institute for Tropical Diseases (NITD) for the initial construct of the dengue virus protease. Funding by the Australian Research Council is gratefully acknowledged.

## References

- 1 Bhatt S, Gething PW, Brady OJ, Messina JP, Farlow AW, Moyes CL, Drake JM, Brownstein JS, Hoen AG, Sankoh O, Myers MF, George DB, Jaenisch T, Wint GR, Simmons CP, Scott TW, Farrar JJ & Hay SI (2013) The global distribution and burden of dengue. *Nature* **496**, 504-507.
- 2 Kuno G (2007) Research on dengue and dengue-like illness in East Asia and the Western Pacific during the first half of the 20<sup>th</sup> century. *Rev Med Virol* **17**, 327-341.
- 3 Guzman MG, Halstead SB, Artsob H, Buchy P, Farrar J, Gubler DJ, Hunsperger E, Kroeger A, Margolis HS, Martínez E, Nathan MB, Pelegrino JL, Simmons C, Yoksan S & Peeling RW (2010) Dengue: a continuing global threat. *Nat Rev Microbiol* **8**, S7-S16.
- 4 Lescar J, Luo D, Xu T, Sampath A, Lim SP, Canard B & Vasudevan SG (2008) Towards the design of antiviral inhibitors against flaviviruses: the case for the multifunctional NS3 protein from dengue virus as a target. *Antiviral Res* **80**, 94-101.
- 5 Yusof R, Clum S, Wetzel M, Murthy HMK & Padmanabhan R (2000) Purified NS2B/NS3 serine protease of dengue virus type 2 exhibits cofactor NS2B dependence for cleavage of substrates with dibasic amino acids *in vitro*. *J Biol Chem* **275**, 9963-9969.
- 6 Preugschat F, Yao CW & Strauss JH (1990) In vitro processing of dengue virus type 2 nonstructural proteins NS2A, NS2B, and NS3. *J Virol* **64**, 4364-4374.
- 7 Leung D, Schroder K, White H, Fang NX, Stoermer MJ, Abbenante G, Martin JL, Young PR & Fairlie DP (2001) Activity of recombinant dengue 2 virus NS3 protease in the presence of a truncated NS2B co-factor, small peptide substrates, and inhibitors. *J Biol Chem* **276**, 45762-45771.
- 8 Erbel P, Schiering N, D'Arcy A, Rénatus M, Kroemer M, Lim SP, Yin Z, Keller TH, Vasudevan SG & Hommel U (2006) Structural basis for the activation of flaviviral NS3 proteases from dengue and West Nile virus. *Nat Struct Mol Biol* **13**, 372-373.
- 9 Chandramouli S, Joseph JS, Daudenarde S, Gatchalian J, Cornillez-Ty C & Kuhn P (2010) Serotype-specific structural differences in the protease-cofactor complexes of the dengue virus family. *J Virol* **84**, 3059-3067.
- 10 Wu PSC, Ozawa K, Lim SP, Vasudevan S, Dixon NE & Otting G (2007) Cell-free transcription/translation from PCR amplified DNA for high-throughput NMR studies. *Angew Chem Int Ed* **46**, 3356-3358.
- 11 de la Cruz L, Nguyen THD, Ozawa K, Shin J, Graham B, Huber T & Otting G (2011) Binding of low-molecular weight inhibitors promotes large conformational changes in the dengue virus NS2B-NS3 protease: fold analysis by pseudocontact shifts. *J Am Chem Soc* **133**, 19205-19215.
- 12 Li J, Lim SP, Beer D, Patel V, Wen D, Tumanut C, Tully DC, Williams JA, Jiricek J, Priestle JP, Harris JL & Vasudevan SG (2005) Functional profiling of recombinant NS3 proteases from all four serotypes of dengue virus using tetrapeptide and octapeptide substrate libraries. *J Biol Chem* **280**, 28766-28774.
- 13 Yin Z, Patel SJ, Wang WL, Wang G, Chan WL, Rao KRR, Alam J, Jeyaraj DA, Ngew X, Patel V, Beer D, Lim SP, Vasudevan SG & Keller TH (2006) Peptide inhibitors of dengue virus NS3 protease. Part 1: warhead. *Bioorg Med Chem Lett* **16**,

36-39.

- 14 Yin Z, Patel SJ, Wang WL, Chan WL, Rao KRR, Wang G, Ngew X, Patel V, Beer D, Knox JE, Ma NL, Ehrhardt C, Lim SP, Vasudevan SG & Keller TH (2006) Peptide inhibitors of dengue virus NS3 protease. Part 2: SAR study of tetrapeptide aldehyde inhibitors. *Bioorg Med Chem Lett* **16**, 40-43.
- 15 Bodenreider C, Beer D, Keller TH, Sonntag S, Wen D, Yap L, Yau YH, Geifman Shochat S, Huang D, Zhou T, Caflisch A, Su XC, Ozawa K, Otting G, Vasudevan SG, Lescar J & Lim SP (2009) A fluorescence quenching assay to discriminate between specific and non-specific inhibitors of dengue virus protease. *Anal Biochem* **395**, 195-204.
- 16 Tomlinson SM, Malmstrom RD, Russo A, Mueller N, Pang YP & Watowich SJ (2010) Structure-based discovery of dengue virus protease inhibitors. *Antiviral Res* **82**, 110-114.
- 17 Tomlinson SM & Watowich SJ (2011) Anthracene-based inhibitors of dengue virus NS2B-NS3 protease. *Antiviral Res* **89**, 127-135.
- 18 Steuer C, Gege C, Fischl W, Heinonen KH, Bartenschlager R & Klein CD (2011) Synthesis and biological evaluation of  $\alpha$ -ketoamides as inhibitors of the dengue virus protease with antiviral activity in cell-culture. *Bioorg Med Chem* **19**, 4067-4074.
- 19 Knehans T, Schüller A, Doan DN, Nacro K, Hill J, Güntert P, Madhusudhan MS, Weil T & Vasudevan SG (2011) Structure-guided fragment-based in silico drug design of dengue protease inhibitors. *J Comput Aided Mol Des* **25**, 263-274.
- 20 Schüller A, Yin Z, Chia CSB, Doan DN, Kim HK, Shang L, Loh TP, Hill J & Vasudevan SG (2011) Tripeptide inhibitors of dengue and West Nile virus NS2B-NS3 protease. *Antiviral Res* **92**, 96-101.
- 21 Yang CC, Hsieh YC, Lee SJ, Wu SH, Liao CL, Tsao CH, Chao YS, Chern JH, Wu CP & Yueh A (2011) Novel dengue virus-specific NS2B/NS3 protease inhibitor, BP2109, discovered by a high-throughput screening assay. *Antimicrob Agents Chemother* **55**, 229-238.
- 22 Nitsche C, Steuer C & Klein CD (2011) Arylcianoacrylamides as inhibitors of the dengue and West Nile virus proteases. *Bioorg Med Chem* **19**, 7318-7337.
- 23 Doan DN, Li KQ, Basavannacharya C, Vasudevan SG & Madhusudhan MS (2012) Transplantation of a hydrogen bonding network from West Nile virus protease onto dengue-2 protease improves catalytic efficiency and sheds light on substrate specificity. *Protein Eng Des Sel* **25**, 843-850.
- 24 Rothan HA, Han HC, Ramasamy TS, Othman S, Rahman NA & Yusof R (2012) Inhibition of dengue NS2B-NS3 protease and viral replication in Vero cells by recombinant retrocyclin-1. *BMC Infect Dis* **12**, 314.
- 25 Tomlinson SM & Watowich SJ (2012) Use of parallel validation high-throughput screens to reduce false positives and identify novel dengue NS2B-NS3 protease inhibitors. *Antiviral Res* **93**, 245-252.
- 26 Xu S, Li H, Shao X, Fan C, Ericksen B, Liu J, Chi C & Wang C (2012) Critical effect of peptide cyclization on the potency of peptide inhibitors against dengue virus NS2B-NS3 protease. *J Med Chem* **55**, 6881-6887.

- 27 Nitsche C, Behnam MA, Steuer C & Klein CD (2012) Retro peptide-hybrids as selective inhibitors of the dengue virus NS2B-NS3 protease. *Antiviral Res* **94**, 72-79.
- 28 Pasfield LA, de la Cruz L, Ho J, Coote ML, Otting G & McLeod MD (2013) Synthesis of ( $\pm$ )-panduratin A and related natural products using the high pressure Diels-Alder reaction. *Asian J Org Chem* **2**, 60-63.
- 29 Aleshin AE, Shiryaev SA, Strongin AY & Liddington RC (2007) Structural evidence for regulation and specificity of flaviviral proteases and evolution of the Flaviviridae fold. *Protein Sci* **16**, 795-806.
- 30 Noble CG, Seh CC, Chao AT & Shi PY (2012) Ligand-bound structures of the dengue virus protease reveal the active conformation. *J Virol* **86**, 438-446.
- 31 Robin G, Chappell K, Stoermer MJ, Hu S, Young PR, Fairlie DP & Martin JL (2009) Structure of West Nile virus NS3 protease: ligand stabilization of the catalytic conformation. *J Mol Biol* **385**, 1568-1577.
- 32 Hammamy MZ, Haase C, Hammami M, Hilgenfeld R & Steinmetzer T (2013) Development and characterization of new peptidomimetic inhibitors of the West Nile virus NS2B-NS3 protease. *ChemMedChem* **8**, 231-241.
- 33 Falgout B, Miller RH & Lai C-J (1993) Deletion analysis of dengue virus type 4 nonstructural protein NS2B: Identification of a domain required for NS2B-NS3 protease activity. *J Virol* **67**, 2034-2042.
- 34 Wu CF, Wang SH, Sun CM, Hu ST & Syu WJ (2003) Activation of dengue protease autocleavage at the NS2B-NS3 junction by recombinant NS3 and GST-NS2B fusion proteins. *J Virol Method* **114**, 45-54.
- 35 Niyomrattanakit P, Winoyanu wattikun P, Chanprapaph S, Angsuthanasombat C, Panyim S & Katzenmeier G (2004) Identification of residues in the dengue virus type 2 NS2B cofactor that are critical for NS3 protease activation. *J Virol* **78**, 13708-13716.
- 36 Phong WY, Moreland NJ, Lim SP, Wen D, Paradkar PN & Vasudevan SG (2011) Dengue protease activity: the structural integrity and interaction of NS2B with NS3 protease and its potential as a drug target. *Biosci Rep* **31**, 399-409.
- 37 Radichev I, Shiryaev SA, Aleshin AE, Ratnikov BI, Smith JW, Liddington RC & Strongin AY (2008) Structure-based mutagenesis identifies important novel determinants of the NS2B cofactor of the West Nile virus two-component NS2B-NS3 proteinase. *J Gen Virol* **89**, 636-641.
- 38 Su XC, Ozawa K, Qi R, Vasudevan SG, Lim SP & Otting G (2009) NMR analysis of the dynamic exchange of the NS2B cofactor between open and closed conformations of the West Nile virus NS2B-NS3 protease. *PLoS Negl Trop Dis* **3**, e561.
- 39 Kim YM, Gayen S, Kang C, Joy J, Huang Q, Chen AS, Wee JL, Ang MJ, Lim HA, Hung AW, Li R, Noble CG, Lee le T, Yip A, Wang QY, Chia CS, Hill J, Shi PY & Keller TH (2013) NMR analysis of a novel enzymatically active unlinked dengue NS2B-NS3 protease complex. *J Biol Chem* **288**, 12891-12900.

- 40 Bai Y, Milne JS, Mayne L & Englander SW (1993) Primary structure effects on peptide group hydrogen exchange. *Proteins* **17**, 75-86.
- 41 Chappell KJ, Stoermer MJ, Fairlie DP & Young PR (2008) Mutagenesis of the West Nile virus NS2B cofactor domain reveals two regions essential for protease activity. *J Gen Virol* **89**, 1010–1014.
- 42 Ghanesh VK, Muller N, Judge K, Luan CH, Padmanabhan R & Murthy KHM (2005) Identification and characterization of nonsubstrate based inhibitors of the essential dengue and West Nile virus proteases. *Bioorg Med Chem* **13**, 257-264.
- 43 Frecer V & Miertus S (2010) Design, structure-based focusing and in silico screening of combinatorial library of peptidomimetic inhibitors of Dengue virus NS2B-NS3 protease. *J Comput Aided Mol Des* **24**, 195-212.
- 44 Tambunan USF & Alamudi S (2010) Designing cyclic peptide inhibitor of dengue virus NS3-NS2B protease by using molecular docking approach. *Bioinformation* **5**, 250-254.
- 45 Frimayanti N, Chee CF, Zain SM & Rahman NA (2011) Design of new competitive dengue Ns2b/Ns3 protease inhibitors – a computational approach. *Int J Mol Sci* **12**, 1089-1100.
- 46 Lai H, Prasad GS, Padmanabhan (2013) Characterization of 8-hydroxyquinoline derivatives containing aminobenzothiazole as inhibitors of dengue virus type 2 protease *in vitro*. *Antivir Res* **97**, 74-80.
- 47 Prusis P, Junaid M, Petrovska R, Yahorava S, Yahorau A, Katzenmeier G, Lapins M & Wikberg JE (2013) Design and evaluation of substrate-based octapeptide and non substrate-based tetrapeptide inhibitors of dengue virus NS2B-NS3 proteases. *Biochem Biophys Res Commun* **434**, 767-772.
- 48 Wichapong K, Nueangaudom A, Pianwanit S, Sippl W & Kokpol S (2013) Identification of potential hit compounds for Dengue virus NS2B/NS3 protease inhibitors by combining virtual screening and binding free energy calculations. *Trop Biomed* **30**, 388-408.
- 49 Nitsche C, Schreier VN, Behnam MA, Kumar A, Bartenschlager R & Klein CD (2013) Thiazolidinone-peptide hybrids as dengue virus protease inhibitors with antiviral activity in cell culture. *J Med Chem* **56**, 8389-8403.
- 50 Pambudi S, Kawashita N, Phanthanawiboon S, Omokoko MD, Masrinoul P, Yamashita A, Limkittikul K, Yasunaga T, Takagi T, Ikuta K & Kurosu T (2013) A small compound targeting the interaction between nonstructural proteins 2B and 3 inhibits dengue virus replication. *Biochem Biophys Res Commun* **440**, 393-398.
- 51 Yildiz M, Ghosh S, Bell JA, Sherman W & Hardy JA (2013) Allosteric inhibition of the NS2B-NS3 protease from dengue virus. *ACS Chem Biol* **8**, 2744-2742.
- 52 Zhou GC, Weng Z, Shao X, Liu F, Nie X, Liu J, Wang D, Wang C & Guo K (2013) Discovery and SAR studies of methionine-proline anilides as dengue virus NS2B-NS3 protease inhibitors. *Bioorg Med Chem Lett* **23**, 6549-6554.
- 53 Su XC, Ozawa K, Yagi H, Lim SP, Wen D, Ekonomiuk D, Huang D, Keller TH, Sonntag S, Caflisch A, Vasudevan SG & Otting G (2009) NMR study of complexes between low-molecular weight inhibitors and the West Nile virus NS2B-NS3 protease. *FEBS J* **276**, 4244-4255.

- 54 Ekonomiuk D, Su XC, Ozawa K, Bodenreider C, Lim SP, Yin Z, Keller TH, Beer D, Patel V, Otting G, Caflisch A & Huang D (2009) Discovery of a non-peptidic inhibitor of West Nile virus NS2B-NS3 protease by high-throughput docking. *PLoS Negl Top Dis* **3**, e356.
- 55 Kang C & Gayen S (2013) Exploring the binding of peptidic West Nile virus NS2B-NS3 protease inhibitors by NMR. *Antivir Res* **97**, 137-144.
- 56 Arakaki TL, Fang NX, Fairlie DP, Young PR & Martin JL (2002) Catalytically active Dengue virus NS3 protease forms aggregates that are separable by size exclusion chromatography. *Prot Expr Purif* **25**, 241-247.
- 57 Otting G (2008) Prospects for lanthanides in structural biology by NMR. *J Biomol NMR* **42**, 1-9.
- 58 Sivashanmugam A, Murray V, Cui C, Zhang Y, Wang J & Li Q (2009) Practical protocols for production of very high yields of recombinant proteins using *Escherichia coli*. *Protein Sci* **18**, 936-948.
- 59 Schoepfer R (1993) The pRSET family of T7 promoter expression vectors for *Escherichia coli*. *Gene* **124**, 83-85.
- 60 Neylon C, Brown SE, Kralicek AV, Miles CS, Love CA & Dixon NE (2000) Interaction of the *Escherichia coli* replication terminator protein (Tus) with DNA: a model derived from DNA-binding studies of mutant proteins by surface plasmon resonance. *Biochemistry* **39**, 11989-11999.
- 61 Graham B, Loh CT, Swarbrick JD, Ung P, Shin J, Yagi H, Jia X, Chhabra S, Pintacuda G, Huber T & Otting G (2011) A DOTA-amide lanthanide tag for reliable generation of pseudocontact shifts in protein NMR spectra. *Bioconj Chem* **22**, 2118-2125.
- 62 Ozawa K, Wu PCS, Dixon NE & Otting G (2006) <sup>15</sup>N-labelled proteins by cell free protein synthesis: strategies for high-throughput NMR studies of proteins and protein-ligand complexes. *FEBS J* **273**, 4154-4159.
- 63 Apponyi M, Ozawa K, Dixon NE & Otting G (2008) Cell-free protein synthesis for analysis by NMR spectroscopy. *Methods Mol Biol* **426**, 257-268.
- 64 Ozawa K, Headlam MJ, Schaeffer PM, Henderson BR, Dixon NE & Otting G (2004) Optimization of an *Escherichia coli* system for cell-free synthesis of selectively <sup>15</sup>N-labelled proteins for rapid analysis by NMR spectroscopy. *Eur J Biochem* **271**, 4084-4093.
- 65 Su XC, Loh CT, Qi R & Otting G (2011) Suppression of isotope scrambling in cell-free protein synthesis by broadband inhibition of PLP enzymes for selective <sup>15</sup>N-labelling and production of perdeuterated proteins in H<sub>2</sub>O. *J Biomol NMR* **50**, 35-42.
- 66 Ekonomiuk D, Su XC, Ozawa K, Bodenreider C, Lim SP, Otting G, Huang D & Caflisch A (2009) Flaviviral protease inhibitors identified by fragment-based library docking into a structure generated by molecular dynamics. *J Med Chem* **52**, 4860-4868.
- 67 Hwang TL, van Zijl PCM & Mori S (1998) Accurate quantitation of water-amide proton exchange rates using the phase-modulated CLEAN Chemical Exchange (CLEANEX-PM) approach with a Fast-HSQC (FHSQC) detection scheme. *J*

*Biomol NMR* **11**, 221-226.

68 Bertini I, Luchinat C & Parigi G (2002) Magnetic susceptibility in paramagnetic NMR. *Prog NMR Spectrosc* **40**, 249–273.

## Figures

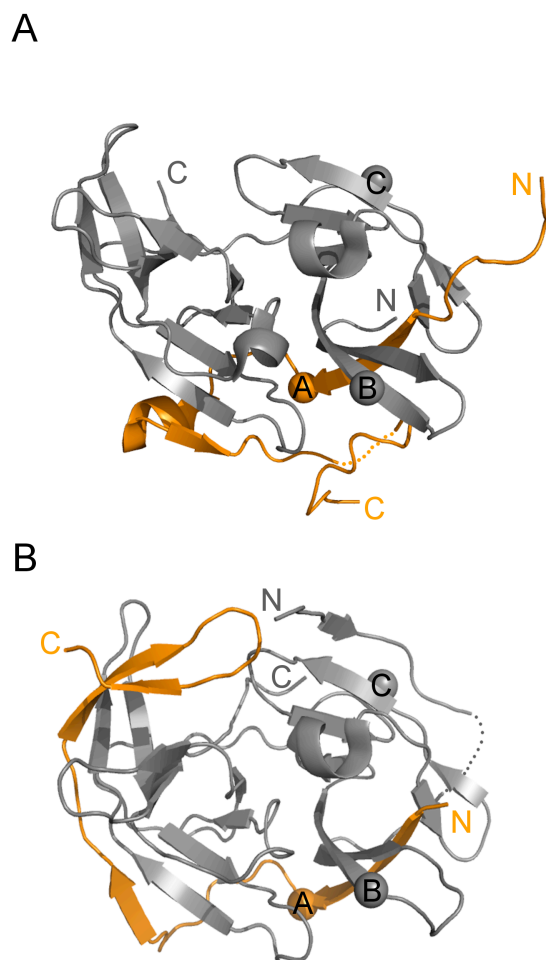


**Fig. 1.** Open and closed conformations observed in crystal structures of the NS2B-NS3 protease from dengue virus serotypes 2 and 3, respectively. In the orientation shown, the C- and N-terminal  $\beta$ -barrels of the protease are in the left and right halves, respectively. The parts from NS2B and NS3 are shown in orange and grey, respectively, and their N- and C-termini are labeled. Spheres identify the  $C^{\alpha}$  atoms of the single cysteine residues for the attachment of lanthanide binding tags in the mutants A-C. Dotted lines indicate missing electron density in the crystal structure. (A) Open conformation (PDB ID 2FOM [8]). The C-terminal segment of NS2B, NS2Bc, is far from the active site. (B) Closed conformation (PDB ID 3U1I [30]). NS2Bc wraps around the active site.

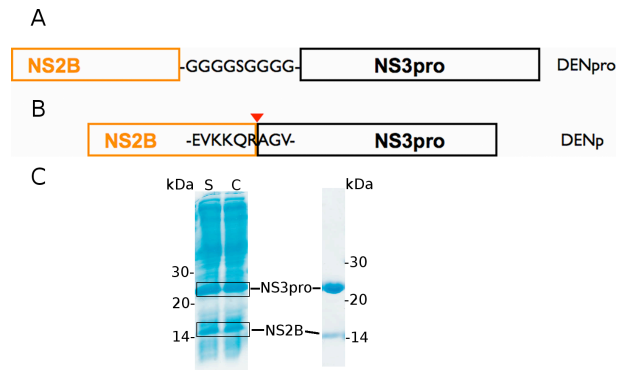


**Fig. 2.** Expression constructs of the dengue virus protease with and without covalent linker between NS2B and NS3. (A) Schematic representation of the protease construct with NS2B (orange) linked to NS3pro (black) via a flexible Gly<sub>4</sub>-Ser-Gly<sub>4</sub> linker. We refer to this construct as DENpro. (B) Same as (A), except that the Gly<sub>4</sub>-Ser-Gly<sub>4</sub> linker is replaced by the natural cleavage site between NS2B and NS3 in dengue virus serotype 2 (EVKKQR). We refer to this construct as DENp. The autoproteolytic cleavage site is identified by a red triangle. See Fig. S1 for the detailed amino acid sequence. (C) SDS-PAGE of DENp with Coomassie blue staining. Left panel: result from cell-free expression (S: supernatant, C: crude reaction mixture); right panel: purified product from *in vivo* expression. In both cases, soluble DENp was obtained without covalent linkage between NS2B and NS3pro. The bands of NS2B and NS3pro are indicated.

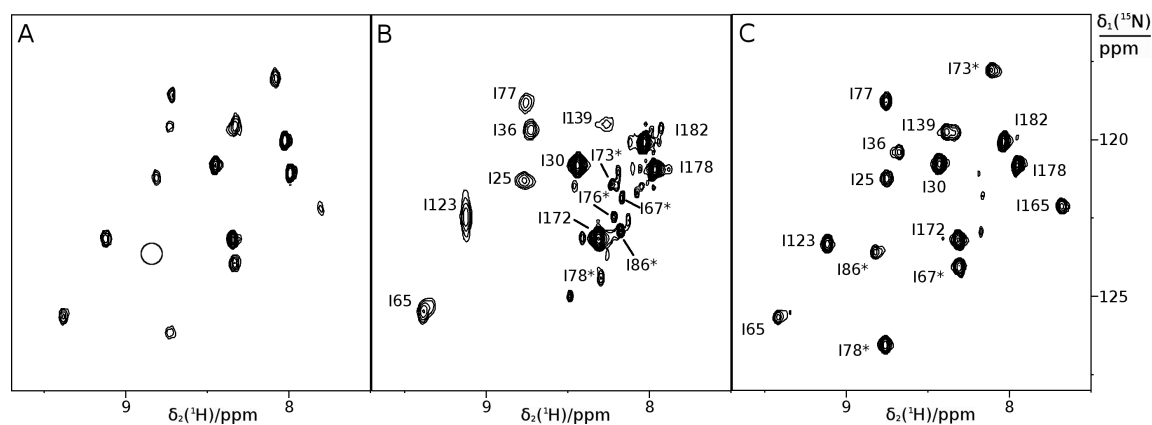


**Fig. 3.** Chemical shift conservation suggests that DENp predominantly assumes the closed conformation in the absence of an inhibitor. The spectra show the spectral region of the backbone amides in  $^{15}\text{N}$ -HSQC spectra recorded of selectively  $^{15}\text{N}$ -isoleucine labelled samples of DENp and DENpro. All spectra were acquired using 0.2 mM protein solutions in 90%  $\text{H}_2\text{O}/10\%$   $\text{D}_2\text{O}$  with 20 mM MES, pH 6.5, 50 mM NaCl at 25 °C on a Bruker 800 MHz NMR spectrometer. Assignments of NS2B are identified by stars. (A)  $^{15}\text{N}$ -HSQC spectrum of DENp. The circle indicates the position of the cross-peak of Ile86\* which was observed with very weak intensity in a spectrum of a different sample. (B) Same as (A), except for DENpro. Weak narrow cross-peaks of NS2B appearing at random coil chemical shifts are from a minor species of variable intensity between different sample preparations. (C) Same as (B), except that a 5-fold excess of inhibitor **1** was added to induce the closed conformation.

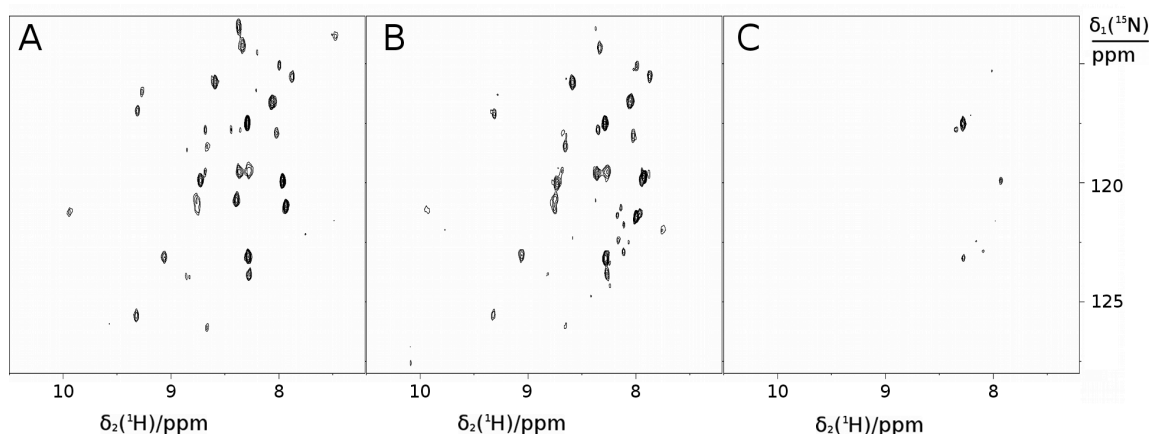


**Fig. 4.** Reduced peak intensities in the  $^{15}\text{N}$ -HSQC spectra are caused by conformational, not chemical exchange. All spectra were recorded of selectively  $^{15}\text{N}$ -Ser and  $^{15}\text{N}$ -Ile labelled DENp, using the same sample condition and spectrometer as in Fig. 3. See Fig. S4 for resonance assignments. (A)  $^{15}\text{N}$ -HSQC spectrum at pH 6.5. (B) Same as (A), except that the pH was 7.5. (C)  $^{15}\text{N}$ -HSQC exchange spectrum at pH 7.5. The experiment was recorded with the CLEANEX-PM-FHSQC pulse sequence [62], in which selective water excitation by a 7.5 ms  $180^\circ$  pulse sequence was followed by 60 ms CLEANEX-PM mixing prior to the conventional HSQC pulse sequence. Cross-peaks in this spectrum arise from magnetisation transfer from water to amide protons by proton exchange.

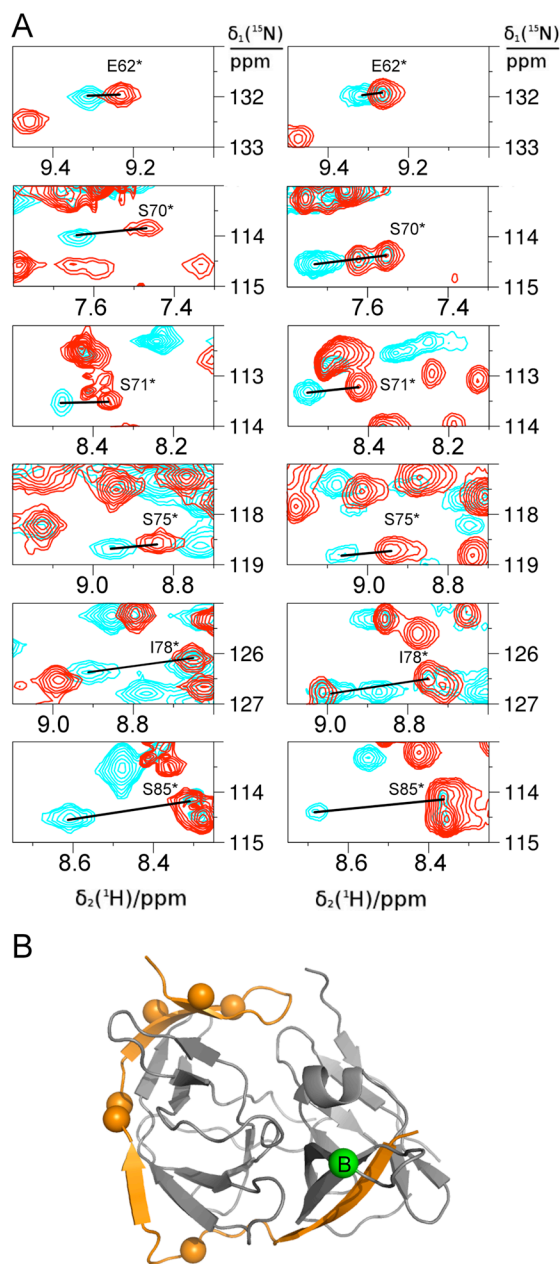


**Fig. 5.** Similar PCSs are observed for NS2B of DENp without inhibitor as for DENpro with inhibitor 1. The spectra were recorded on a 600 MHz NMR spectrometer using the same conditions as in Fig. 3. (A) Superimpositions of selected spectral regions of  $^{15}\text{N}$ -HSQC spectra of mutant B of DENp without inhibitor (left panels) and DENpro with inhibitor **1** (right panels). The samples were tagged with the C2-tag loaded with paramagnetic  $\text{Tb}^{3+}$  (cyan peaks) or diamagnetic  $\text{Y}^{3+}$  (red peaks). (B) Cartoon representation of the dengue virus protease in the closed conformation (PDB ID 3U1I [30]), showing NS2B in orange and NS3pro in grey. The locations of the residues

analysed in (A) are highlighted by balls and the site of the C2-tag is indicated by a green sphere.

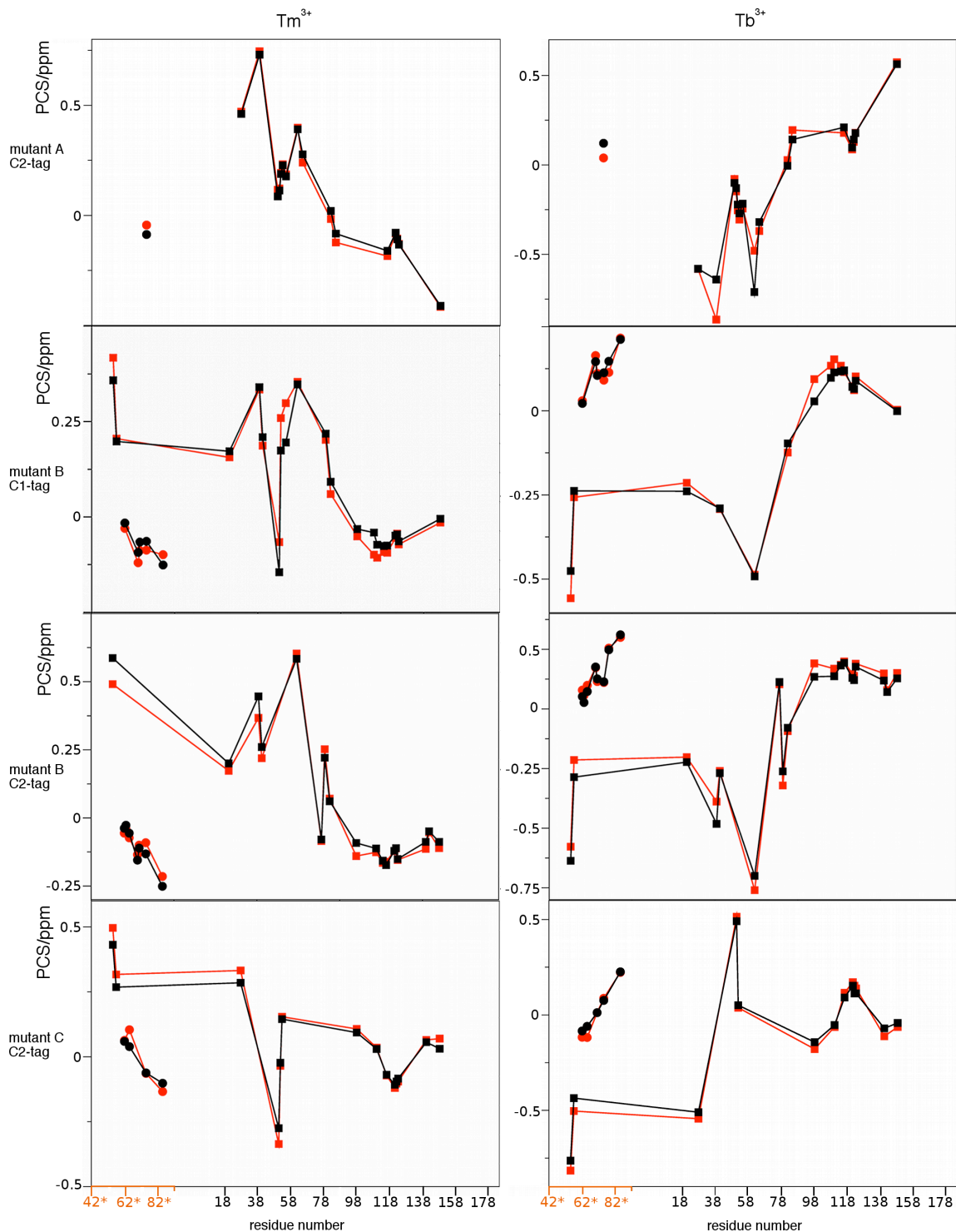


**Fig. 6.** PCSs demonstrate that DENp assumes a closed conformation very similar to that reported in the crystal structure of DENpro with bound inhibitor [30]. The figure plots the PCSs measured with different tags and metal ions for mutants A, B and C of DENp

in the absence of inhibitor (red symbols) and DENpro in the presence of inhibitor **1** (black symbols). Squares identify the PCSs of NS3pro and NS2B residues that form part of the N-terminal  $\beta$ -barrel of NS3pro; these residues are structurally similar between open and closed conformations (see Fig. 1). PCSs for NS2Bc are shown as circles. For clarity, data are shown only for residues for which PCSs could be measured both for DENp and DENpro. The close similarity between the PCSs indicates closely similar structures.

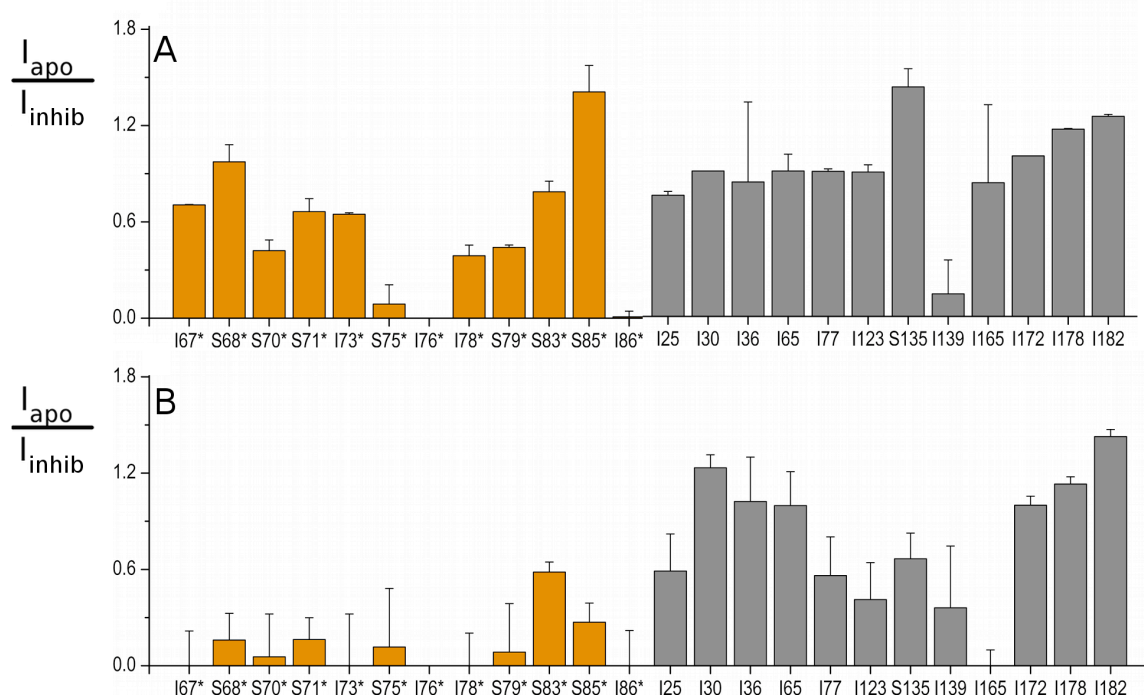


**Fig. 7.** Ratios of cross-peak heights in  $^{15}\text{N}$ -HSQC spectra of DENp and DENpro without and with inhibitor **1** provide evidence for conformational exchange. All spectra were measured at pH 6.5 under the same sample conditions as in Fig. 3. In each spectrum, the cross-peak intensities were determined relative to the intense cross-peak of Ile172. Error ranges were estimated from the reproducibility of the peak heights in spectra recorded with two different samples, taking into account the level of white noise. Data for residues of NS2B and NS3 are shown in orange and grey, respectively. Residues, for which cross-peaks at or near the position characteristic of the closed conformation could not be observed in the absence of inhibitor are reported with a peak intensity ratio of zero. (A) Data for DENp. (B) Data for DENpro.

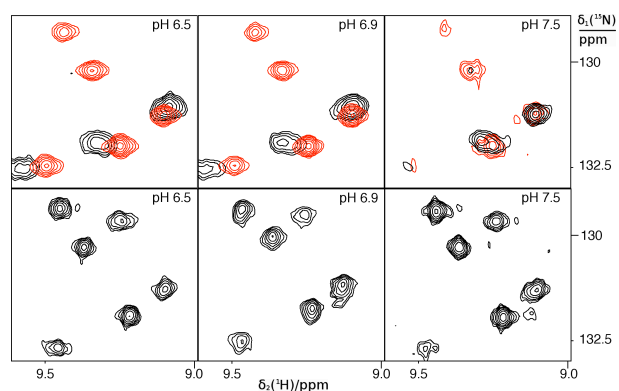


**Fig. 8.** The conformational equilibria in DENp and DENpro are pH dependent. Top panel: Superimposition of a selected spectral region from  $^{15}\text{N}$ -HSQC spectra of DENp (red) and DENpro (black) recorded without inhibitor at different pH. Except for the pH, the sample conditions were the same as in Fig. 3. The decrease in peak intensities with increasing pH indicates increasing population of alternative conformations with chemical shifts different from the closed state of the protease. Bottom panel: Corresponding region of DENpro in complex with inhibitor **1**, providing a reference for the closed conformation.

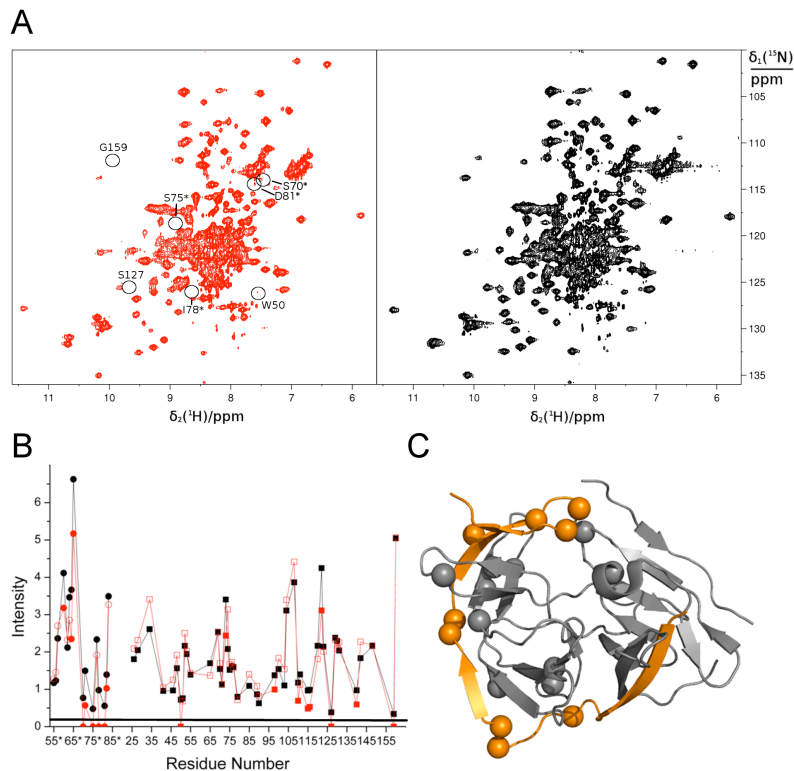


**Fig. 9.** High ionic strength weakens the association between NS2Bc and NS3pro. (A)  $^{15}\text{N}$ -HSQC spectra of uniformly  $^{15}\text{N}$ -labelled DENp at 300 mM NaCl (red spectrum) and 30 mM NaCl (black spectrum). All other sample conditions were the same as in Fig. 3. Circles identify peaks that broadened beyond detection after the addition of sodium chloride. (B) Cross-peak heights observed in the spectra of (A) plotted versus the amino acid sequence. Red and black symbols correspond to the data measured at high and low salt concentrations, respectively. A horizontal line indicates the level of white noise in the spectrum at high salt. Circles and squares refer to NS2B and NS3, respectively. The peaks in DENp displaying intensity reductions greater than 20% after the addition of salt are highlighted by filled red symbols. (C) Cartoon representation of the NS2B-NS3 protease in the closed conformation with NS2B and NS3 shown in orange and grey, respectively. Spheres identify the residues highlighted in (B) for greatly reduced peak intensities upon addition of salt.

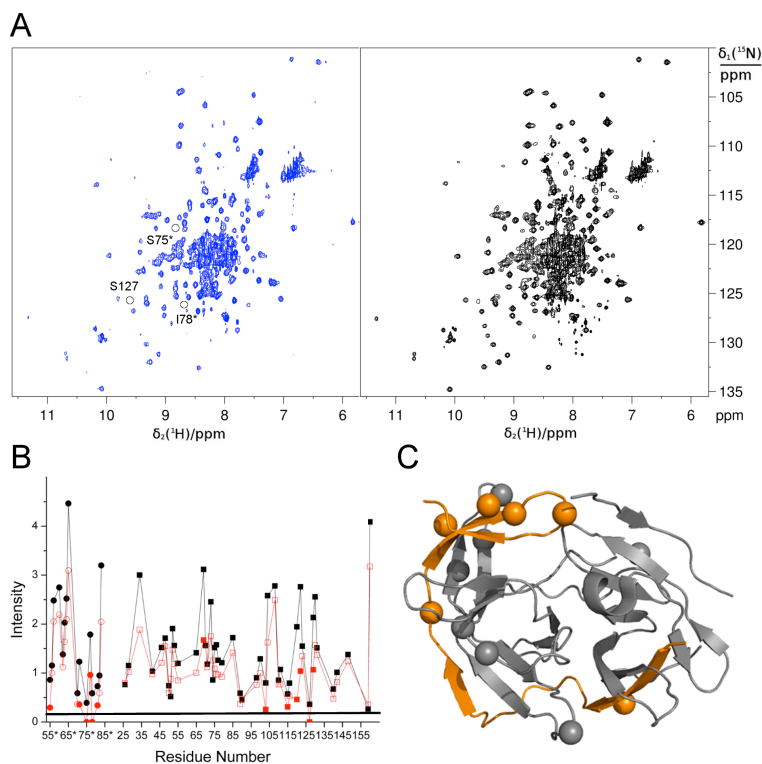


**Fig. 10.** High pH weakens the association between NS2Bc and NS3pro. The figure corresponds to Fig. 9, except that the peaks affected by pH rather than salt are analysed. (A) <sup>15</sup>N-HSQC spectra of uniformly <sup>15</sup>N-labelled DENp at pH 7.5 (blue spectrum) and pH 6.5 (black spectrum). All other sample conditions were the same as in Fig. 3. Circles identify peaks that broadened beyond detection at pH 7.5. (B) Cross-peak heights observed in the spectra of (A) plotted versus the amino acid sequence. Red and black symbols correspond to the data measured at high and low pH, respectively. A horizontal line indicates the level of white noise in the spectrum at high pH. Intensities are in arbitrary units and the spectra were scaled to give similar intensities for the peaks with highest intensities. The peaks in DENp displaying intensity reductions greater than 40% at high pH are highlighted by filled red symbols. (C) Cartoon representation of the NS2B-NS3 protease in the closed conformation with NS2B and NS3 shown in orange and grey, respectively. Spheres identify the residues highlighted in (B) for substantial reductions in peak intensities at pH 7.5.

## Supporting Information

### Binding mode of the activity-modulating C-terminal segment of NS2B to NS3 in the dengue virus NS2B-NS3 protease

Laura de la Cruz, Wan-Na Chen, Bim Graham, Gottfried Otting

	51*	61*	71*	81*	91*
DENV1	<i>AD LSLEKAAEVS</i>	<i>WEEEAHSGA</i>	<i>SHNILVEVQD</i>	<i>DGTMKIKDEE</i>	<i>RDDTLTILLK</i>
DENV2	<b>AD LELERAADV</b>	<b>WEEQAIEISGS</b>	<b>SPILSITISE</b>	<b>DGSMSIKNEE</b>	<b>EEQTLTILIR</b>
DENV3	<i>AD LTVKAADV</i>	<i>WEEEAEQTGV</i>	<i>SHNLMITVDD</i>	<i>DGTMRIKDEE</i>	<i>TENILTVLLK</i>
DENV4	<i>AD LSLEKAANVQ</i>	<i>WDEMADITGS</i>	<i>SPIIEVKQDE</i>	<i>DGSFSIRDVE</i>	<i>ETNMITLLVK</i>
	101*	111*	121*	1	11
DENV1	<i>ATLLAVSGVY</i>	<i>PLSIPATLFV</i>	<i>WYFWQKKKQR</i>	<i>SGVLWDTPSP</i>	<i>PEVERAVLDD</i>
DENV2	<i>TGLLVISGLF</i>	<i>PASIPITAAA</i>	<b>WYLW<b>EVKKQR</b></b>	<b>AGVLWDVPSP</b>	<b>PPVGKAELED</b>
DENV3	<i>TALLIVSGIF</i>	<i>PYSIPATLLV</i>	<i>WHTWQKQTOR</i>	<i>SGVLWDVPSP</i>	<i>PETQKAELEE</i>
DENV4	<i>LALITVSGLY</i>	<i>PLAIPVTMTL</i>	<i>WYMWQVKTQR</i>	<i>SGALWDVPSP</i>	<i>AAAQKATLTE</i>
	21	31	41	51	61
DENV1	<i>GIYRIMQRGL</i>	<i>LGRSQVGVGV</i>	<i>FQDGVFHTMW</i>	<i>HVTRGAVLMY</i>	<i>QGKRLEPSWA</i>
DENV2	<b>GAYRIKQKGI</b>	<b>LGYSQIGAGV</b>	<b>YKEGTFHTMW</b>	<b>HVTRGAVLMH</b>	<b>KGKRIEPSWA</b>
DENV3	<i>GVYRIKQQGI</i>	<i>FGKTQVGVGV</i>	<i>QKEGVFHTMW</i>	<i>HVTRGAVLTH</i>	<i>NGKRLEPNWA</i>
DENV4	<i>GVYRIMQRGL</i>	<i>FGKTQVGVGI</i>	<i>HMEGVFHTMW</i>	<i>HVTRGSVICH</i>	<i>ESGRLEPSWA</i>
	71	81	91	101	111
DENV1	<i>SVKKDLISYG</i>	<i>GGWRFQGSWN</i>	<i>TGEEVQVIAV</i>	<i>EPGKNPKNVQ</i>	<i>TAPGTFKTPE</i>
DENV2	<b>DVKKDLISYG</b>	<b>GGWKLEGEWK</b>	<b>EGEEVQVLAL</b>	<b>EPGKNPRAVQ</b>	<b>TKPGLFKTNT</b>
DENV3	<i>SVKKDLISYG</i>	<i>GGWRLSAQWQ</i>	<i>KGEEVQVIAV</i>	<i>EPGKNPKNFQ</i>	<i>TMPGIFQTTT</i>
DENV4	<b>DVRNDMISYG</b>	<b>GGWRLGDKWD</b>	<b>KEEDVQVLAI</b>	<b>EPGKNPKHVQ</b>	<b>TKPGLFKTLT</b>
	121	131	141	151	161
DENV1	<i>GEVGAIALDF</i>	<i>KPGTSGSPIV</i>	<i>NREGKIVGLY</i>	<i>GNGVVTTSGT</i>	<i>YVSAIAQAKA</i>
DENV2	<b>GTIGAVSLDF</b>	<b>SPGTSGSPIV</b>	<b>DKKGKVVGLY</b>	<b>GNGVVTRSGA</b>	<b>YVSAIAQTEK</b>
DENV3	<i>GEIGAIALDF</i>	<i>KPGTSGSPII</i>	<i>NREGKVVGLY</i>	<i>GNGVVTKNGG</i>	<i>YVSGIAQTNA</i>
DENV4	<i>GEIGAVTLDF</i>	<i>KPGTSGSPII</i>	<i>NRKGVVIGLY</i>	<i>GNGVVTKSGD</i>	<i>YVSAITQAER</i>
	171				
DENV1	<i>SQEGPLPEIE</i>	<i>DEVFRK</i>			
DENV2	<b>SIED-NPEIE</b>	<b>DDIFRK</b>			
DENV3	<i>EPDGPTPELE</i>	<i>EEMFKK</i>			
DENV4	<i>IGEP-DYEVD</i>	<i>EDIFRK</i>			

**Figure S1. Sequence alignment of the NS2B-NS3pro in the dengue virus serotypes 1-4** (NCBI taxonomy IDs 11053, 11070, 408693 and 408688). Positively and negatively charged amino acids are shown in blue and red, respectively. Residues of NS2B are displayed in italics and identified by an asterisk. NS2B contains a hydrophilic domain acting as a cofactor (residues 49\*-95\*) followed by a hydrophobic transmembrane

domain and a C-terminal hydrophilic segment containing the autoproteolytic cleavage site (residues 125\*-130\*) leading to NS3. In previous studies of the dengue virus protease, the NS2B cofactor was linked to NS3pro via a covalent Gly<sub>4</sub>-Ser-Gly<sub>4</sub>-linker, a construct referred to as DENpro [1]. The construct presented here, referred to as DENp, uses the autoproteolytic cleavage site (residues 125\*-130\*) instead of the Gly<sub>4</sub>-Ser-Gly<sub>4</sub>-linker to connect NS2B and NS3pro. The resulting amino acid sequence of the DENp construct is shown in bold, underlined residues form the catalytic triad. Autoproteolysis of DENp during protein expression yields a non-covalent, active protease complex.

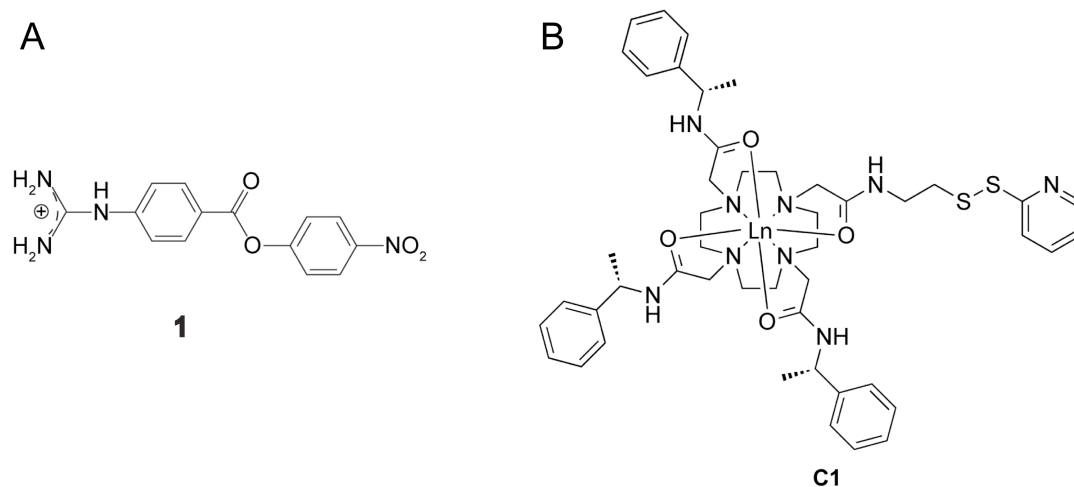


**Figure S2. Chemical structures of inhibitor 1 and C1 lanthanide tag.** (A) Inhibitor used in the present work. It is a generic inhibitor of serine proteases [2,3], which reacts with the protease with formation of an ester bond to Ser135, releasing yellow *p*-nitrophenolate [4]. (B) Structure of the C1 tag with bound lanthanide ion [5]. The tag is activated by a pyridin-2-yl-disulfanyl group for spontaneous reaction with a cysteine thiol group to form a disulfide bond. The C2-tag is the opposite enantiomer of the C1-tag with ((**R**)-1-phenylethyl)acetamide pendants instead of ((**S**)-1-phenylethyl)acetamide pendants throughout.

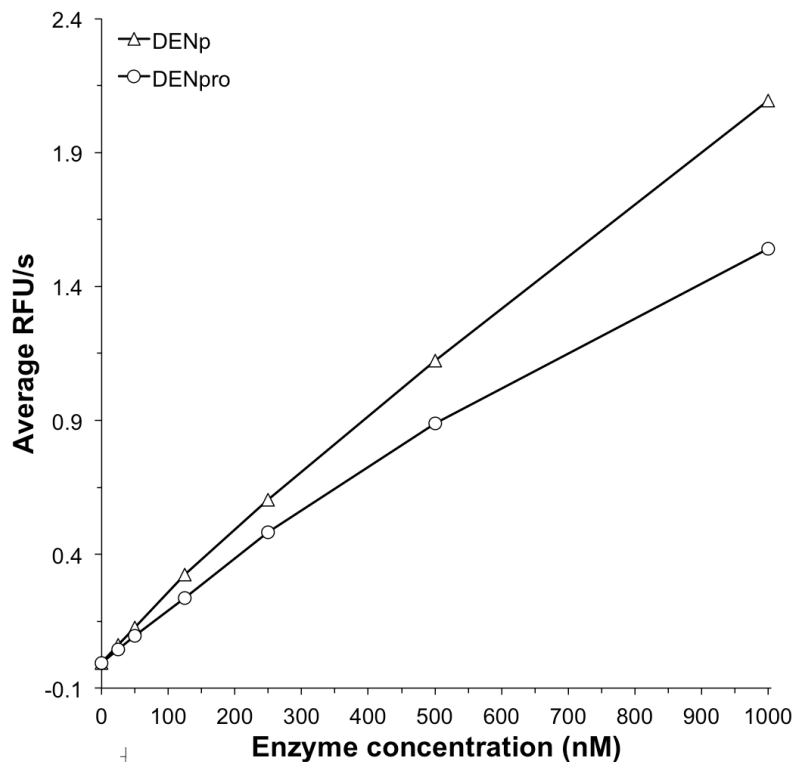


**Figure S3. DENp is enzymatically active.** The activities of DENp (triangles) and DENpro (circles) were compared using 10  $\mu$ M Bz-norleucine-lysine-arginine-arginine-AMC [6] in 50 mM Tris·HCl (pH 7.5), 50 mM NaCl and 1 mM CHAPS in a final volume of 50  $\mu$ L at 25 °C. The proteolytic reaction was monitored by the increase in fluorescence (relative fluorescence units per second, exciting at 380 nm and monitoring the emission at 450 nm) observed during 30 mins on a SpectraMax microplate reader. Each measurement was performed in three different wells and the data were averaged.

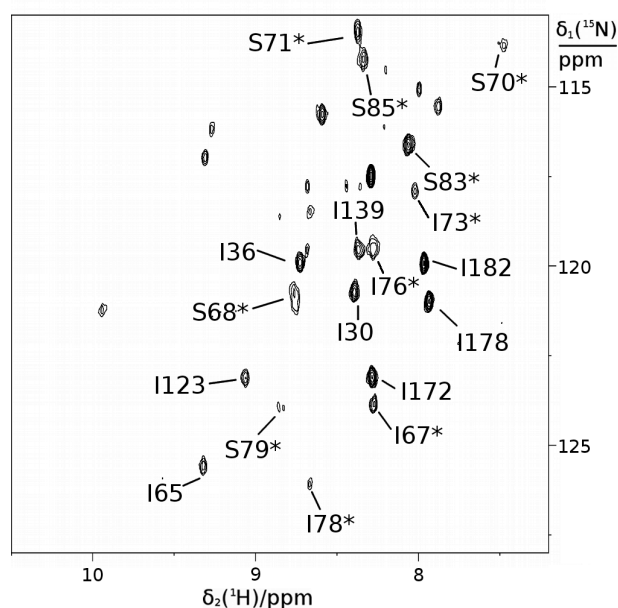


**Figure S4.**  $^{15}\text{N}$ -HSQC spectrum of DENp selectively labelled with  $^{15}\text{N}$ -serine and  $^{15}\text{N}$ -isoleucine. Same as Figure 3A, except that the resonance assignments are shown.

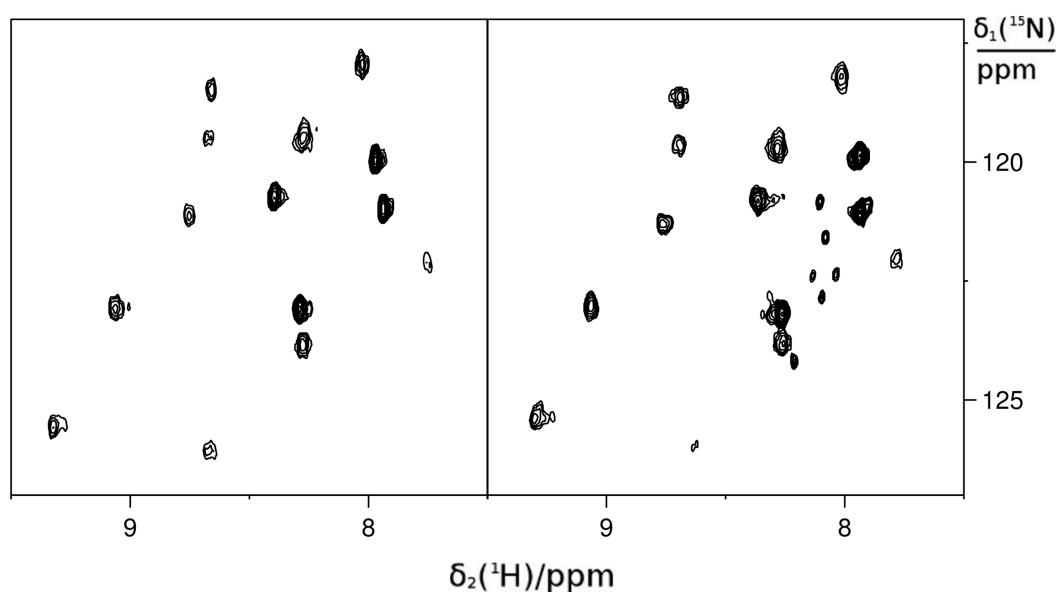


**Figure S5.**  $^{15}\text{N}$ -HSQC spectra of DENp selectively labelled with  $^{15}\text{N}$ -isoleucine at different ionic strengths. Both spectra were acquired using 0.2 mM protein solutions in 90%  $\text{H}_2\text{O}/10\%$   $\text{D}_2\text{O}$  with 20 mM MES, pH 6.5, at 25 °C on a Bruker 800 MHz NMR spectrometer. (A)  $^{15}\text{N}$ -HSQC spectrum recorded in the presence of 50 mM NaCl. The spectrum is the same as the spectrum in Figure 3A. (B) Same as (A), except that the buffer contained 300 mM NaCl.

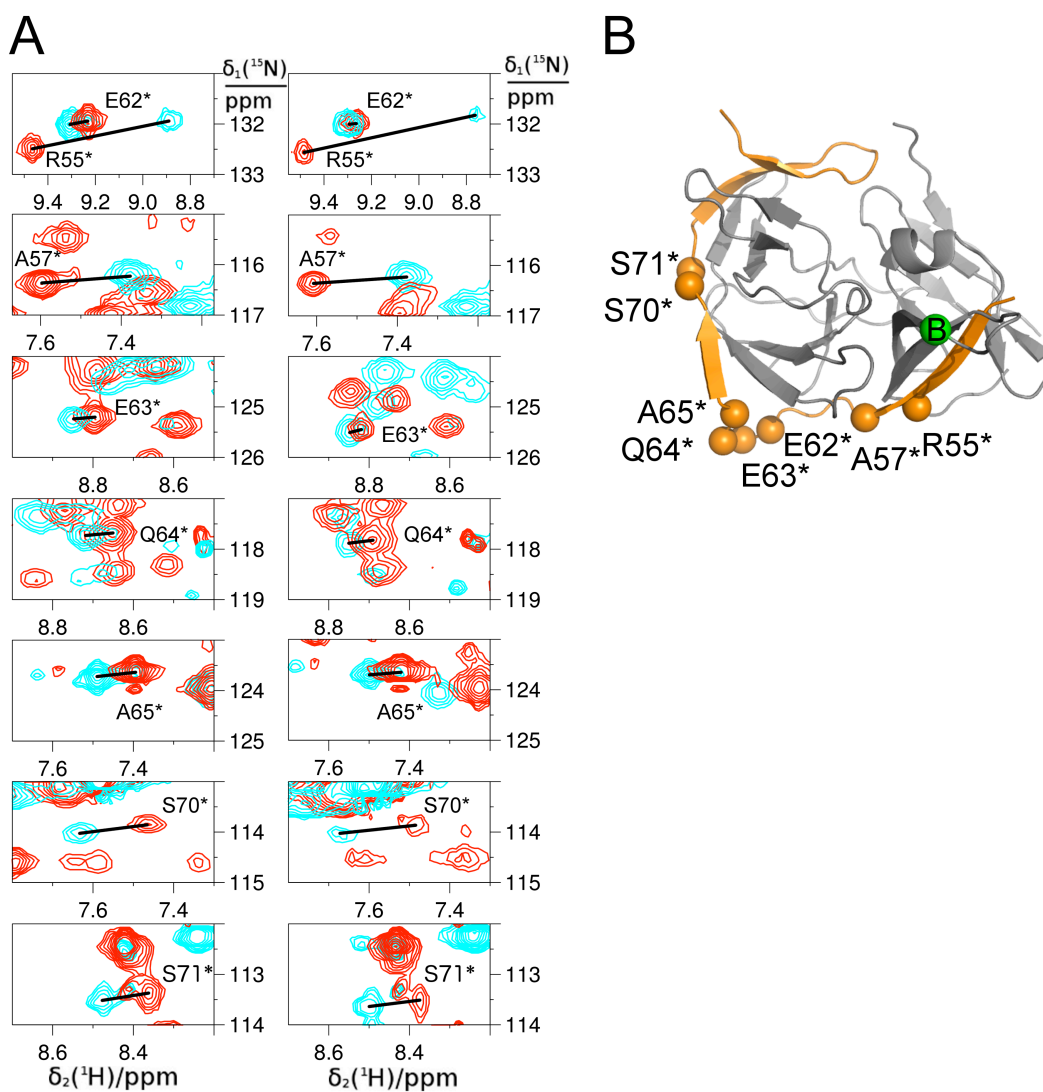


**Figure S6. PCSs observed for NS2B of DENp at 50 mM and 300 mM NaCl.** The spectra were recorded using the same conditions as in Figure 3. (A) Superimpositions of selected spectral regions of  $^{15}\text{N}$ -HSQC spectra of mutant B of DENp with the C2 tag at 50 mM NaCl (left panels) and 300 mM NaCl (right panels). The samples were tagged with the C2-tag loaded with paramagnetic  $\text{Tb}^{3+}$  (cyan peaks) or diamagnetic  $\text{Y}^{3+}$  (red peaks). The resonance assignments of the selected cross-peaks are indicated. (B) Cartoon representation of the dengue virus protease in the closed conformation (PDB ID 3U1I [7]), showing NS2B in orange and NS3pro in grey. The locations of the residues analysed in (A) are highlighted by balls and the site of the C2-tag is indicated by a green sphere.

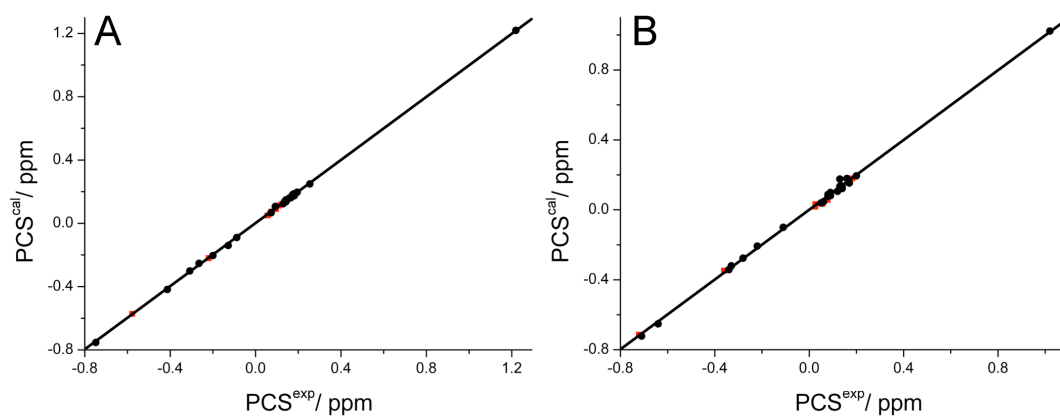


**Figure S7. Correlations between back-calculated and experimental PCSs of DENp at low and high salt.** The PCSs were measured for the backbone amide protons of a uniformly  $^{15}\text{N}$ -labelled cysteine mutant of DENp with the cysteine positioned at site B (see Figure 1) and ligated with either a paramagnetic C2-Tb $^{3+}$  or a diamagnetic C2-Y $^{3+}$  tag. The PCSs of NS2B and NS3pro are shown as red squares and black circles, respectively. NS2B appears to be located in the same position at high and low salt, as this point fits equally well to the correlation line under both conditions. (A) Data at 50 mM NaCl. (B) Data at 300 mM NaCl.

**Table S1.** PCSs of backbone amide protons of  $^{15}\text{N}$ -labelled DENp mutant B with C2-tag loaded with  $\text{Tb}^{3+}$  at 50 mM and 300 mM NaCl concentrations<sup>a</sup>

Residue <sup>b</sup>	PCS in low salt (ppm)	PCS in high salt (ppm)
Arg55*	-0.578	-0.722
Ala57*	-0.220	-0.361
Glu62*	0.075	0.026
Glu63*	0.056	0.026
Gln64*	0.070	0.056
Ala65*	0.096	0.078
Ser70*	0.169	0.183
Ser71*	0.119	0.140
Ser75*	0.108	-
Gly21	-0.200	-0.280
Gly39	-0.413	-0.640
Thr41	-0.265	-0.340
Thr48	-0.128	-0.220
His51	1.219	1.020
Gly62	-0.748	-0.710
Asp71	0.254	0.200
Ile77	0.092	0.060
Tyr79	-0.308	-0.330
Gly82	-0.088	-0.110
Leu98	0.175	0.090
Ala108	0.142	0.080
Gln110	0.166	0.140
Thr111	0.158	0.130
Gly114	0.179	0.130
Phe116	0.195	0.160
Gly121	0.141	0.140
Thr122	0.130	0.120
Ile123	0.181	0.170
Val140	0.135	0.090
Lys142	0.073	0.050
Gly148	0.143	0.080

<sup>a</sup> Other parameters were 20 mM MES, pH 6.5, 800 MHz  $^1\text{H}$  NMR frequency. PCSs were calculated as the difference in chemical shifts measured with paramagnetic  $\text{Tb}^{3+}$  minus the chemical shifts with diamagnetic  $\text{Y}^{3+}$ .

<sup>b</sup> NS2B residues are identified by an asterisk.

**Table S2.**  $\Delta\chi$  tensor parameters of DENp mutant B with C2-Tb<sup>3+</sup> tag<sup>a</sup>

	$\Delta\chi_{ax}$	$\Delta\chi_{rh}$	x	y	z	$\alpha$	$\beta$	$\gamma$
Low salt	-16.1 (0.6)	-1.5 (0.3)	29.2 (0.2)	34.0 (0.2)	-4.2 (0.3)	7.7 (1.2)	48.4 (1.0)	56.9 (8.7)
High salt	-13.7 (1.1)	-1.4 (0.4)	30.4 (0.3)	34.2 (0.3)	-4.0 (0.4)	20.0 (2.1)	51.2 (1.7)	26.0 (21.5)

<sup>a</sup> The tensor parameters of NS2B-NS3pro complex were calculated with the program Numbat [8], using the PCSs of Table S1 and the model of the closed conformation established previously [4]. This model deviates from the crystal structure of serotype 3 DENpro 3U1I [7] with a backbone RMSD of 0.7 Å. The axial and rhombic components of the  $\Delta\chi$  tensors are given in  $10^{-32}$  m<sup>3</sup> and the Euler angles in degrees, using the zyz convention and unique tensor representation [8]. Error estimates (in brackets) were determined from fits obtained by randomly omitting 10% of the PCS data.

## References

- 1 Leung D, Schroder K, White H, Fang NX, Stoermer MJ, Abbenante G, Martin JL, Young PR & Fairlie DP (2001) Activity of recombinant dengue 2 virus NS3 protease in the presence of a truncated NS2B co-factor, small peptide substrates, and inhibitors. *J Biol Chem* **276**, 45762-45771.
- 2 Chase T & Shaw E (1967) p-Nitrophenyl-p'-guanidinobenzoate HCl: a new active site titrant for trypsin. *Biochem Biophys Res Commun* **29**, 508-514.
- 3 Scheiner CJ & Quigley JP (1982) Detection, identification and partial characterization of serine proteases and esterases in biological systems. *Analyt Biochem* **122**, 58-69.
- 4 de la Cruz L, Nguyen THD, Ozawa K, Shin J, Graham B, Huber T & Otting G (2011) Binding of low-molecular weight inhibitors promotes large conformational changes in the dengue virus NS2B-NS3 protease: fold analysis by pseudocontact shifts. *J Am Chem Soc* **133**, 19205-19215.
- 5 Graham B, Loh CT, Swarbrick JD, Ung P, Shin J, Yagi H, Jia X, Chhabra S, Pintacuda G, Huber T & Otting G (2011) A DOTA-amide lanthanide tag for reliable generation of pseudocontact shifts in protein NMR spectra. *Bioconj Chem* **22**, 2118-2125.
- 6 Löhr K, Knox JE, Phong WY, Ma NL, Yin Z, Sampath A, Patel SJ, Wang WL, Chan WL, Ranga Rao KR, Wang G, Vasudevan SG, Keller TH & Lim SP (2007) Yellow fever virus NS3 protease: peptide-inhibition studies. *J Gen Virol* **88**, 2223-2227.
- 7 Noble CG, Seh CC, Chao AT & Shi PY (2012) Ligand-bound structures of the dengue virus protease reveal the active conformation. *J Virol* **86**, 438-446.
- 8 Schmitz C, Stanton-Cook MJ, Su XC, Otting G & Huber T (2008) Numbat: an interactive software tool for fitting  $\Delta\chi$  tensors to molecular coordinates using pseudocontact shifts. *J Biomol NMR* **41**, 179-189.